Received: 19 December 2022 | Revised: 20 January 2023 | Accepted: 23 January 2023

DOI: 10.1002/ardp.202200663

FULL PAPER

ARCH PHARM DPhG
Archiv der Pharmazie

New benzimidazole-oxadiazole derivatives: Synthesis, α-glucosidase, α-amylase activity, and molecular modeling studies as potential antidiabetic agents

Ulviye Acar Çevik[1] | Ismail Celik[2] | Leyla Paşayeva[3] | Hanifa Fatullayev[2] | Hayrani E. Bostancı[4] | Yusuf Özkay[1] | Zafer A. Kaplancıklı[1]

[1]Department of Pharmaceutical Chemistry, Faculty of Pharmacy, Anadolu University, Eskişehir, Turkey

[2]Department of Pharmaceutical Chemistry, Faculty of Pharmacy, Erciyes University, Kayseri, Turkey

[3]Department of Pharmacognosy, Faculty of Pharmacy, Erciyes University, Kayseri, Turkey

[4]Department of Biochemistry, Faculty of Pharmacy, Sivas Cumhuriyet University, Sivas, Turkey

Correspondence
Ulviye Acar Çevik, Department of Pharmaceutical Chemistry, Faculty of Pharmacy, Anadolu University, Eskişehir 26470, Turkey.
Email: uacar@anadolu.edu.tr

Abstract

Benzimidazole-1,3,4-oxadiazole derivatives (**5a–z**) were synthesized and characterized with different spectroscopic techniques such as ^{1}H NMR, ^{13}C NMR, and HRMS. The synthesized analogs were examined against α-glucosidase and α-amylase enzymes to determine their antidiabetic potential. Compounds **5g** and **5q** showed the most activity with 35.04 ± 1.28 and 47.60 ± 2.16 μg/mL when compared with the reference drug acarbose (IC_{50} = 54.63 ± 1.95 μg/mL). Compounds **5g**, **5o**, **5s**, and **5x** were screened against the α-amylase enzyme and were found to show excellent potential, with IC_{50} values ranging from 22.39 ± 1.40 to 32.07 ± 1.55 μg/mL, when compared with the standard acarbose (IC_{50} = 46.21 ± 1.49 μg/mL). The antioxidant activities of the effective compounds (**5o**, **5g**, **5s**, **5x**, and **5q**) were evaluated by TAS methods. A molecular docking research study was conducted to identify the active site and explain the functions of the active chemicals. To investigate the most likely binding mode of the substances **5g**, **5o**, **5q**, **5s**, and **5x**, a molecular dynamics simulation was also carried out.

KEYWORDS
α-amylase, α-glucosidase, benzimidazole, molecular docking, oxadiazole

1 | INTRODUCTION

Diabetes mellitus (DM) (type 2), is one of the chronic diseases that has seen an alarming increase in prevalence and is a public health problem.[1] The malfunction of insulin secretion and loss of receptivity in the destination organs describe this metabolic disorder. This failure results in blood glucose levels that are higher than anticipated, a condition known as postprandial hyperglycemia, which is an early indicator of diabetes.[2] As a result of untreated or unregulated hyperglycemia, patients with abnormal glucose levels suffer from a variety of long- and short-term concurrent diseases, the most common of which are, cancer,[3,4] cardiovascular diseases,[5] infections[6] as well as increased tumor cell proliferation, amplified metastasis, and repressed tumor cell apoptosis,[7] according to a large number of studies. Along with neuropathy, retinopathy, and nephropathy, there is a decrease in the function of vital body organs.[8]

Inhibition of α-amylase and α-glucosidase has been a key therapy step for effectively controlling DM so far. Anti-α-glucosidase drugs such as acarbose, miglitol, and voglibose (Figure 1) are used to regulate PPHG, although they do not have much α-amylase inhibition capacity and have a lot of side effects.[9–11] The enzyme α-glucosidase is responsible for hydrolysis, transforming unabsorbed oligo- and disaccharides into glucose[12] and restricting the activity of α-glucosidase on dietary carbohydrate absorption and degradation, leading to PPHG suppression.[13] With the pathogenesis and

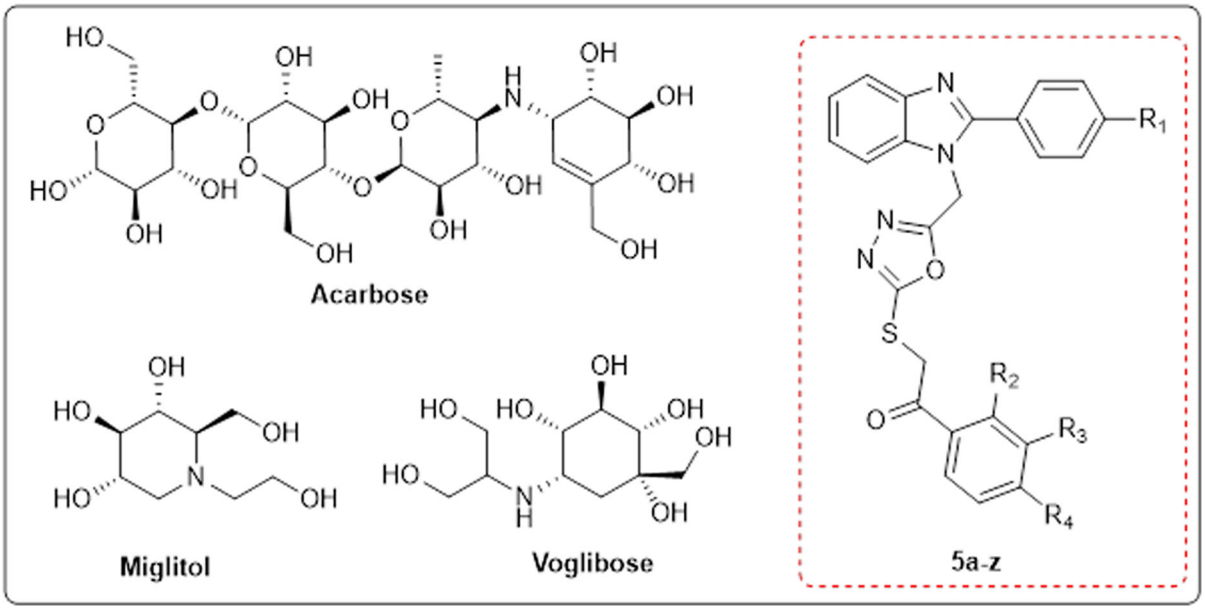

FIGURE 1 Drug molecules used for the treatment of type 2 diabetes mellitus (T2DM); and benzimidazole-oxadiazole hybrids (**5a–z**) designed as inhibitors of α-glucosidase and α-amylase.

maintenance of DM, free radicals cause damage to lipids, proteins, and DNA.[14] Clinical trials have made a relationship between diabetes and breast cancer,[7] and α-glucosidase control has a synergistic therapeutic efficacy in anticancer treatment.[15] The desirable antidiabetic goal should be a therapeutic drug having a safe and competitive inhibitory effect against pancreatic α-amylase and intestinal α-glucosidase to simultaneously decrease and control DM. Several approaches for the synthesis of different heterocycles to regulate the activity of α-amylase and α-glucosidases have recently been discovered. Furthermore, naturally occurring heterocycles derived from medicinal plants have been found to have potent inhibition activity. As a result, much more research is required to develop an effective antidiabetic candidate.[16]

As heterocyclic-based compounds, benzimidazole derivatives are well known as antidiabetic drugs as a result of research into many processes, including peroxisome proliferator, aldose reductase enzyme, activated receptor α-transcriptional activity, dipeptidyl peptidase IV, stearoyl-CoA desaturase, glucokinase, glycosidase receptor, and human glucagon receptor (hGCGR) antagonist.[17,18] Especially, benzimidazole derivatives exhibited α-glucosidase[19–29] and α-amylase[30–33] inhibitor activity; hence, it is important to obtain novel benzimidazole derivatives as antidiabetic compounds. On the other hand, it was reported that oxadiazoles act as a potential class of α-glucosidase[34–41] and α-amylase[42,43] inhibitors. According to several research, oxidative stress significantly contributes to the pathophysiology of both kinds of diabetes mellitus. By nonenzymatic protein glycation, glucose oxidation, and the consequent oxidative breakdown of glycated proteins, free radicals are produced disproportionately in diabetes. Free radical damage to cellular organelles and enzymes, increased lipid peroxidation, and the emergence of insulin resistance can result from abnormally high amounts of free radicals. These oxidative stress-related side effects may encourage the growth of diabetes complications.[44–46]

The goal of this study was to use the molecular hybridization concept of drug development to create active, novel α-glucosidase and α-amylase inhibitor chemical entities. Molecular hybridization is a useful structural modification technique in which two pharmacophoric moieties of a bioactive substance are joined to produce a hybrid molecule that is more effective than the original chemical.[47] This concept can also develop hybrids with a high selectivity profile, minimal side effects, and dual/multiple modes of action.

In the present work, with the aim to have hybrids with improved affinity and efficacy, we combined the oxadiazole moiety with the benzimidazole ring and designed novel analogs (**5a–z**) as Figure 1. The synthetic analogs were tested against α-glucosidase and α-amylase enzymes to determine their antidiabetic potential. The antioxidant activities of the effective compounds were evaluated by TAS methods. In addition, the effects of these compounds on the normal cell line (L929) were evaluated and their cytotoxicity was determined. A molecular docking research study was conducted to identify the active site and explain the functions of the active chemicals.

2 | RESULTS AND DISCUSSION

2.1 | Chemistry

The target benzimidazole-1,3,4-oxadiazole derivatives (**5a–z**) were synthesized as shown in Scheme 1. In the first step, *o*-phenylenediamine with different aldehydes including 4-hydroxybenzaldehyde, 4-methoxybenzaldehyde, and 4-ethoxybenzaldehyde in the presence of sodium metabisulfite in DMF were reacted to afford compounds (**1a–c**).

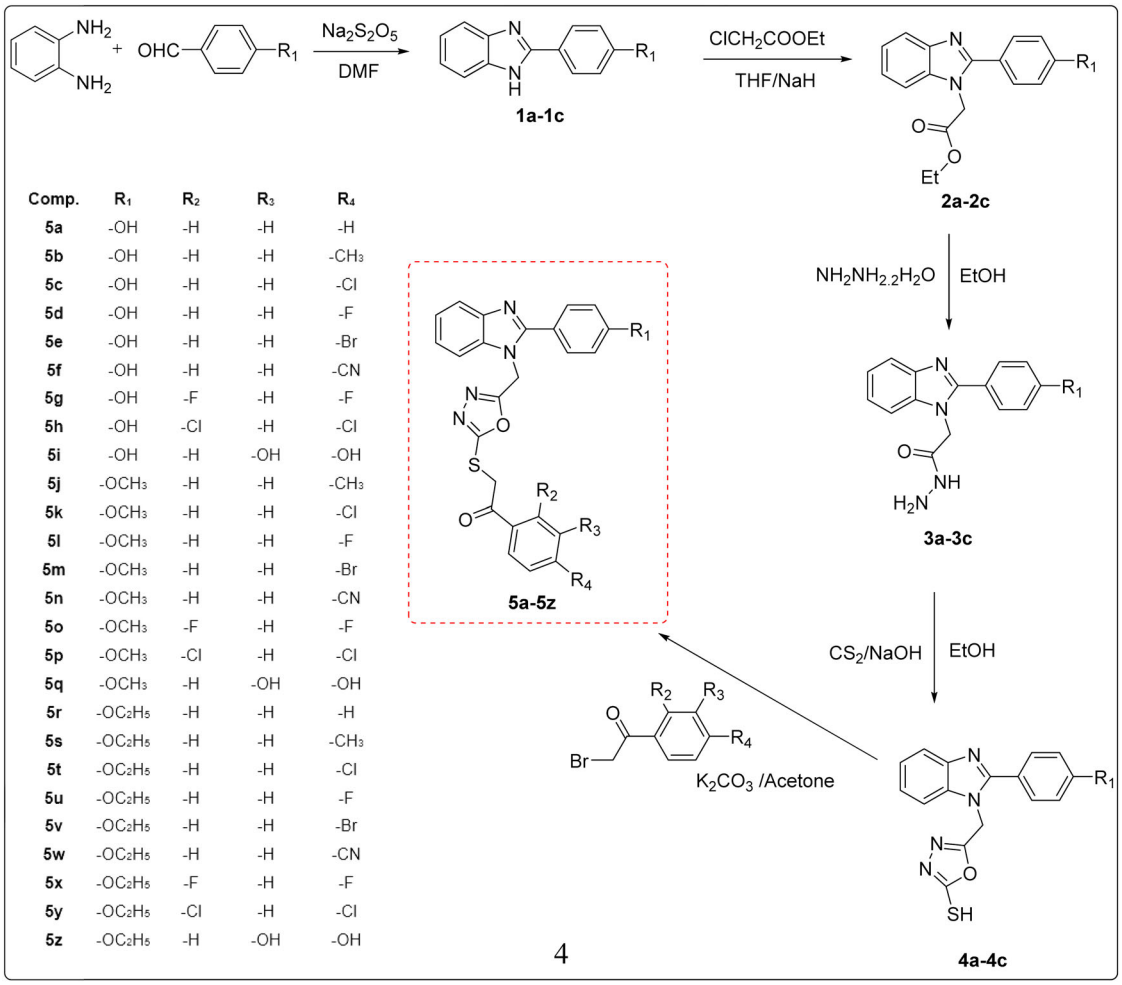

Comp.	R_1	R_2	R_3	R_4
5a	-OH	-H	-H	-H
5b	-OH	-H	-H	$-CH_3$
5c	-OH	-H	-H	-Cl
5d	-OH	-H	-H	-F
5e	-OH	-H	-H	-Br
5f	-OH	-H	-H	-CN
5g	-OH	-F	-H	-F
5h	-OH	-Cl	-H	-Cl
5i	-OH	-H	-OH	-OH
5j	$-OCH_3$	-H	-H	$-CH_3$
5k	$-OCH_3$	-H	-H	-Cl
5l	$-OCH_3$	-H	-H	-F
5m	$-OCH_3$	-H	-H	-Br
5n	$-OCH_3$	-H	-H	-CN
5o	$-OCH_3$	-F	-H	-F
5p	$-OCH_3$	-Cl	-H	-Cl
5q	$-OCH_3$	-H	-OH	-OH
5r	$-OC_2H_5$	-H	-H	-H
5s	$-OC_2H_5$	-H	-H	$-CH_3$
5t	$-OC_2H_5$	-H	-H	-Cl
5u	$-OC_2H_5$	-H	-H	-F
5v	$-OC_2H_5$	-H	-H	-Br
5w	$-OC_2H_5$	-H	-H	-CN
5x	$-OC_2H_5$	-F	-H	-F
5y	$-OC_2H_5$	-Cl	-H	-Cl
5z	$-OC_2H_5$	-H	-OH	-OH

SCHEME 1 General procedure for the synthesis of the final compounds **5a–z**.

To synthesize ethyl 2-(2-(4-substitutedphenyl)-1*H*-benzimidazole-1-yl) acetate derivatives (**2a–c**) and ethyl chloroacetate were mixed in THF, using NaH as a catalyst, and refluxed. The appropriate solution of compounds **2a–c** in ethanol was treated with hydrazine hydrate to prepare 2-(2-(4-substitutedphenyl)-1*H*-benzimidazole-1-yl) acetohydrazide derivatives (**3a–c**). To the mixture of synthesized hydrazide derivatives (**3a–c**) with an aqueous solution of NaOH and ethanol, carbon disulfide was gently added, and compounds (**4a–c**) were obtained. To obtain the final compounds (**5a–z**), a mixture of the compound (**4a–c**) with substituted phenacyl bromide and potassium carbonate was refluxed in acetone for 6 h. Their structures were confirmed by ^{1}H NMR, ^{13}C NMR, and mass spectra.

2.2 | Pharmacology/Biology

2.2.1 | In vitro α-amylase and α-glucosidase inhibition assays

The results of α-amylase and α-glucosidase activities were described in Figures 2–5. Compounds with calculated IC_{50} values are included in Supporting Information: Table S2. According to the results of compounds, the α-amylase inhibitory activity of compounds **5g, 5o, 5s**, and **5x** (***$p < 0.001$) were higher (IC_{50} = 66.94 ± 1.55, 46.74 ± 1.13, 45.08 ± 1.40, and 47.43 ± 3.50 μg/mL, respectively) than acarbose as a positive control. Among these compounds, **5s** were found more active than others. On the other hand, other compounds showed moderate inhibitory activity and the IC_{50} values of compounds namely **5b, 5d, 5h, 5l, 5t, 5u, 5v**, and **5y** cannot be calculated at 1000 μg/mL concentration. Although the results of α-glucosidase showed that compounds **5f, 5g**, and **5q** possessed the highest inhibition effect (***$p < 0.001$) (IC_{50} = 74.27 ± 2.16, 35.04 ± 1.28. and 47.60 ± 2.16 μg/mL). Among these compounds, **5g** and **5q** were found more active than acarbose as a positive control. Additionally, none of the other compounds surpassed the activity of acarbose (IC_{50} = 54.63 ± 1.95 μg/mL) and the IC_{50} value cannot be calculated at 1000 μg/mL concentration. So, according to the results, the compound **5g** displayed the highest inhibitory activity against both α-amylase and α-glucosidase enzymes.

When the effects and structures of the compounds on the alpha-amylase enzyme are examined, it is seen that the presence of the 2,4-difluoro (electron-withdrawing groups) group (compounds **5g**, **5o**, **5x**)

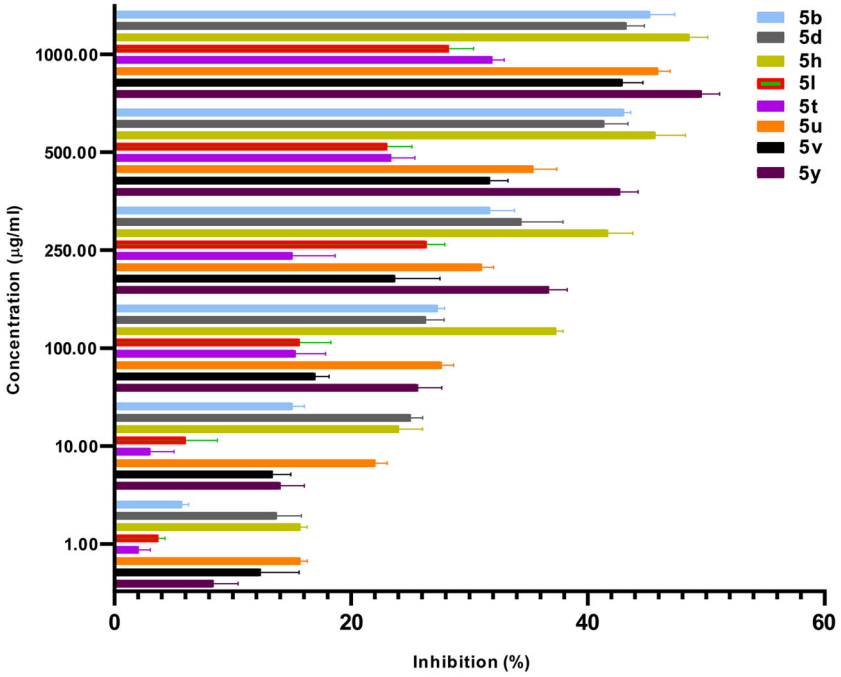

FIGURE 2 α-Amylase inhibitory activities of the compounds (IC_{50} value > 1000).

on the phenyl ring significantly increases the activity. The incorporation of the substituent at the ortho/para position of the phenyl ring enhances the inhibitory activity. The activity is extremely enhanced when the diameter of the added group at the para position is smaller (as in the case of the 2,4-difluorosubstituted derivative). These findings also overlap with previously reported studies.[48] In these compounds, hydroxy, methoxy, and ethoxy groups are located at the 4th position of the phenyl ring attached to benzimidazole. Among them, it was determined that the compound containing the 4-methoxy group (compound **5o**) was more effective. Especially, compound **5s**, which contains a 4-ethoxy group on the phenyl ring attached to benzimidazole, carries methyl group, which is the electron donor group, on the phenyl ring attached to oxadiazole, and it has been determined that it has the highest alpha-amylase activity among the compounds. It was determined that compound **5g** (2-[(5-{[2-(4-hydroxyphenyl)-1*H*-benzimidazole-1-yl] methyl}-1,3,4-oxadiazol-2-yl)thio]-1-(2,4-difluorophenyl)ethan-1-one) was the only compound that was effective on both α-amylase and α-glycosidase enzymes. Among the compounds, compound **5q**, which has the 3,4-dihydroxyphenyl structure, appears to act selectively on the α-glycosidase enzyme.

2.2.2 | Antioxidant activity

The term "high and desired level" refers to total antioxidant capacity values that are greater than or equal to 1.0 mmol Trolox Equiv/L. Total antioxidant capacity values of the compounds **5o**, **5q**, **5g**, **5s**, and **5x** were found high, which is shown in Figure 6 and Supporting Information: Table S2. All of the compounds show high antioxidant properties. In particular, the compound **5x** shows higher Trolox equivalence/L. than vitamin E.

2.2.3 | Cytotoxicity assay

Against the L929 cell line, the cytotoxicity of the compounds **5o**, **5q**, **5g**, **5s**, and **5x** was assessed. To evaluate the cytotoxicity potency of target compounds, the fibroblast cells were treated with the compounds at different concentrations between 6.25 and 100 µM. Cell viability percentages were calculated after the treatment of cells for 24 h. Cytotoxicity results of compounds **5o**, **5q**, **5g**, **5s**, and **5x** against L929 fibroblast are presented in Figure 7 and Supporting Information: Table S3. The maximal dose used caused all compounds to exhibit 60% or more viability.

2.3 | Molecular docking

The molecular docking study was performed to determine the potential interactions and interaction energies of the compounds on α-glucosidase (PDB ID: 5NN8) and α-amylase (PDB ID: 1OSE).[49,50] The three-dimensional structures of α-glucosidase and α-amylase carrying the reference substance acarbose as cocrystal ligand used in enzyme experiments were preferred. For the validation of the molecular docking study, redocking was performed with the acarbose Glide SP contained in 5NN8 and 1OSE, and the RMSD was measured as 1.42 and 2.21 Å, respectively. After molecular docking validation, both target enzymes were docked by the same method as the prepared compounds. The compounds **5a-z** shown in Table S4 gave a docking score between −5.982 and −9.306 kcal/mol, and a Glide emodel docking score between −52.973 and −98.660 kcal/mol against α-glucosidase. The compound with the highest activity against α-glucosidase, **5g**, gave the highest docking interaction energy. The other active compound **5q** formed interaction energy of −7.899 kcal/mol. With the second target

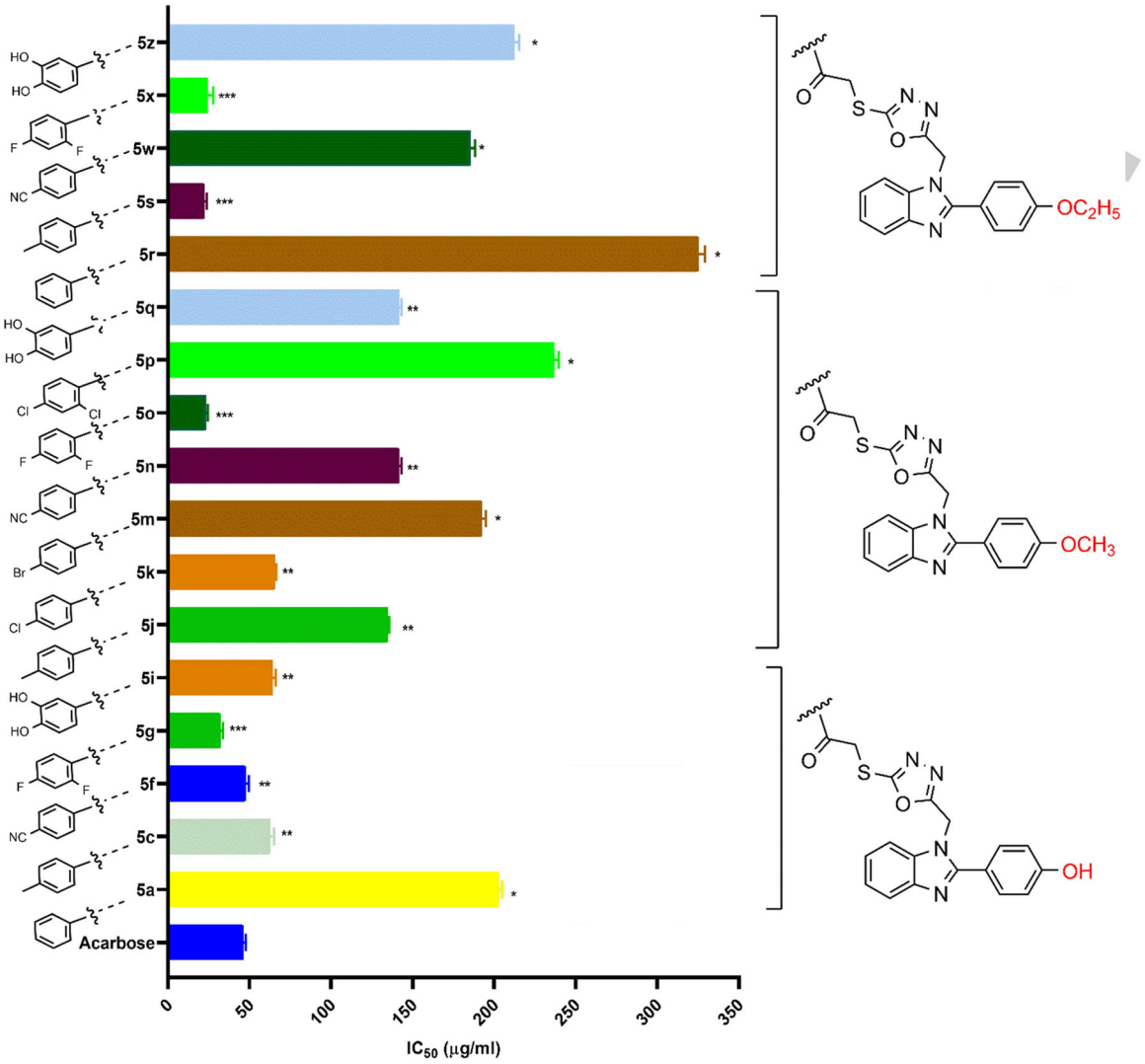

FIGURE 3 α-Amylase IC_{50} values of the compounds. Values are expressed as mean ± SD ($n = 3$). Different asterisk (*) for the same column indicate significant differences at $^{*}p < 0.05$, $^{**}p < 0.001$, and $^{***}p < 0.0001$.

α-amylase, compounds **5a–z** produced a Glide docking score between −5.494 and −7.538 kcal/mol, and a Glide emodel docking score between −71.767 and −93.149 kcal/mol. Among the active compounds, **5o** gave the highest docking score with α-amylase, while the other active compound **5s** gave the lowest docking score.

In protein–ligand atomic interactions, as shown in Figure 8a,b, three conventional H bonds, Phe157 (2.77 Å), Gln350 (2.13 Å), and Asn241 (3.01 Å), Lys155 (2.63 Å), Leu (2.95 Å), and His239 (3.27 Å) halogen bond to fluorine between compound **5g** and α-glucosidase. In addition, compound **5g** gave hydrophobic interactions with Ser156, Pro240, Phe177, Ala278, Glu276, Asp349, and Tyr71. The other active compound **5q** with α-glucosidase created His279 (2.96 Å), His111 (2.68 Å), Arg439 (1.84 Å), Asp68 (1.54 Å and 1.92 Å) H bonds, pi-sulfur interaction with Phe300, and hydrophobic interactions with Phe157, Leu176, Pro240, His245, Ala278, Leu218, Phe177, and Asp214.

Against α-amylase, as shown in Figure 8c–f, dual-acting compound **5g**, Gln63 (2.01 Å) and Lys200 (2.23 Å) with two H bonds and Trp59 (3.06 Å) a fluorinated halogen bond, formed hydrophobic interactions with Asp197, Asp300, Glu233, Tyr62, His305, Val163, and Ile235. Compound **5o**, on the other hand, gave two H bonds with Gln (2.16 and 2.29 Å), hydrophobic interactions with Asp197, Asp300, Glu233, His305, Tyr62, Val163, Trp59, Ile235, and Tyr151 in the α-amylase active pocket. Compound **5s** formed a 2.48 Å length H bond with Tyr151, and Ala307, Ile235, Tyr62, Val163, Trp59, and His305 van der Waals interactions. The other active compound **5x**, on the other hand, formed hydrophobic interactions with Asp197, Asp300, Glu233, Tyr62, Ile235, Leu162, Val163, Trp59, and two H bonds with Tyr151 (2.82 Å) and Gln63 (2.74 Å).

2.4 | Molecular dynamics simulations

MD simulation was performed to examine the stability and interactions of protein–ligand complexes obtained from the molecular docking

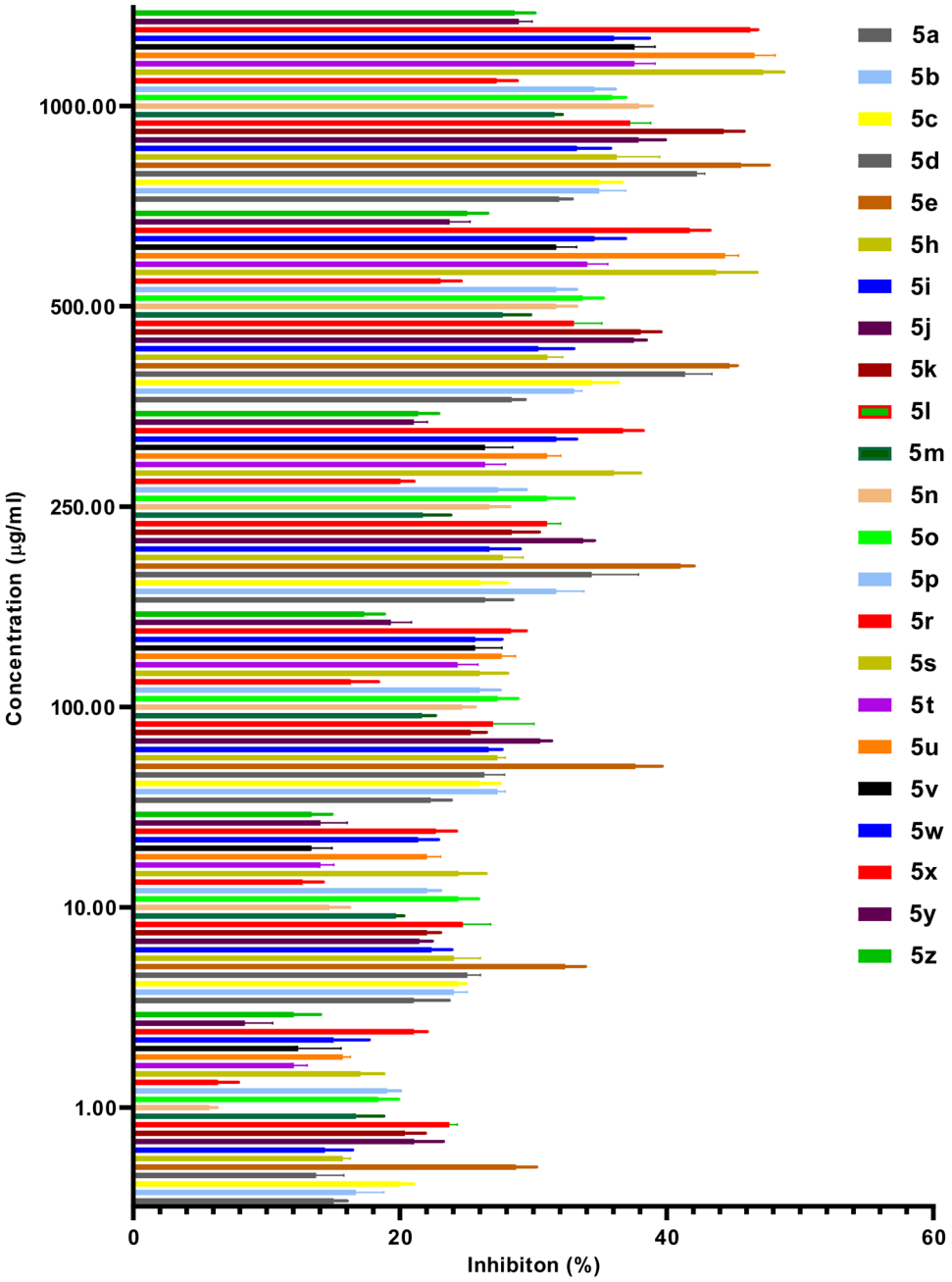

FIGURE 4 α-Glycosidase inhibitory activities of the compounds (IC_{50} value > 1000).

study in silico physiological environment.[51,52] RMSD analysis was performed from the trajectory to show the deviations in protein structure during the 200 ns MD period. Figure 9a shows the RMSD values of the complexes of compounds **5g** and **5q**, which inhibit α-glucosidase more potently than the standard compound acarbose. The A-Glu and **5g** complex was up to 0.6 nm for up to 100 ns and remained stable below 0.8 nm for up to 200 ns. The A-Glu and **5q** complex remained stable below 0.4 nm after the first 20 ns presimulation phase. As shown in Figure 9b, the A-Glu and **5g** complex fluctuated the highest around 0.6 nm, excluding the terminal parts, while the A-Glu and **5q** complex fluctuated below 0.4 nm. According to the RMSD and RMSF plots, the A-Glu and **5q** complex is more stable. Animated video showing interactions of composite **5g** and **5q** creating the active site for 200 ns is provided in Supporting Information: Videos S1 and S2. RMSD and RMSF graphs of the complexes formed by α-amylase of compounds **5g**, **5o**, **5s**, and **5x** are shown in Figure 9c,d. Complexes A-Ami and **5g**, A-Ami and **5o**, A-Ami and **5s**, and A-Ami and **5x** exhibited similar RMSD profiles. According to the RMSF graph, the highest fluctuation occurred around the active site amino acids Tyr151, Val163, and Phe157. A-Ami and **5o** complex showed the highest fluctuation, and A-Ami and **5g** complex showed the lowest fluctuation. An animation showing the movements of the complexes formed with α-amylase of compounds **5g**, **5o**, **5s**, and **5x** during 200 ns MD simulation is provided in Supporting Information: Videos S3-S6.

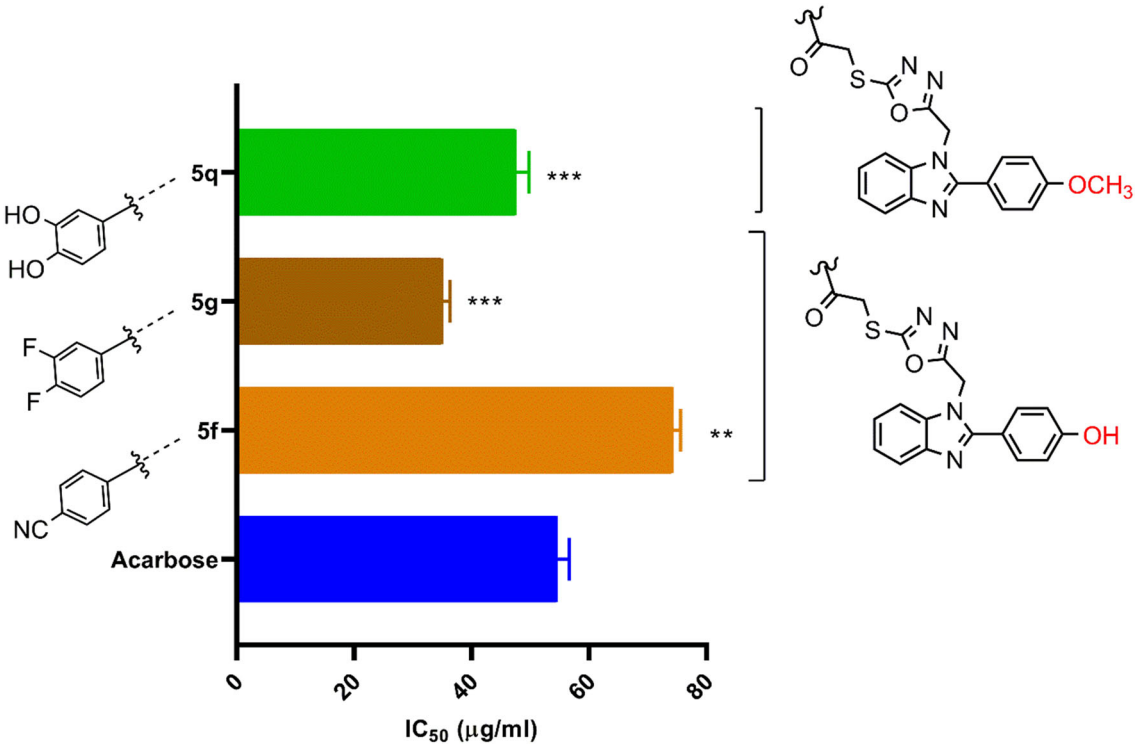

FIGURE 5 α-Glucosidase IC_{50} values of the samples. Values are expressed as mean ± SD (n = 3). Different asterisk (*) for the same column indicate significant differences at $^{**}p < 0.001$ and $^{***}p < 0.0001$.

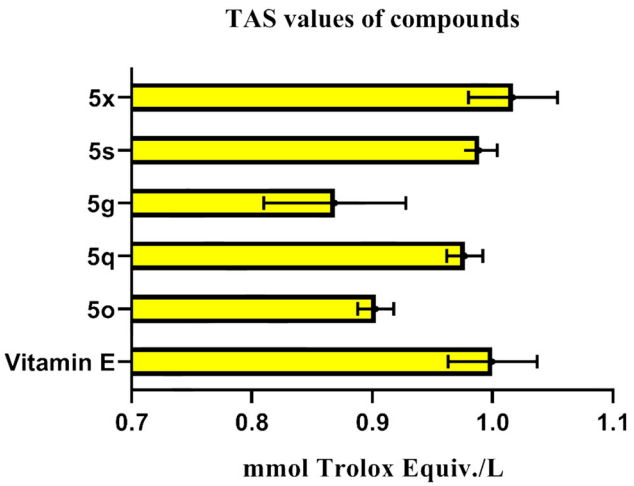

FIGURE 6 Total antioxidant status (TAS) values (mmol Trolox equiv./L).

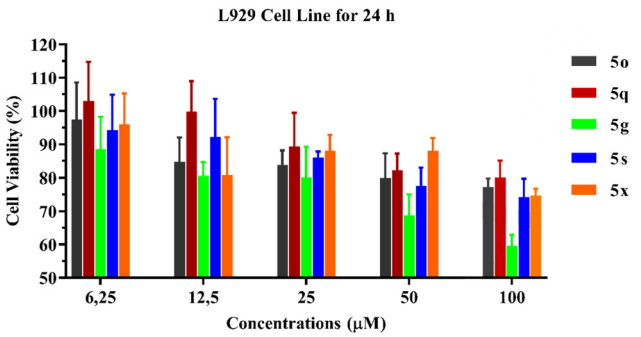

FIGURE 7 After 24 h, % Viability of the L929 cell line.

3 | CONCLUSION

In the present study, benzimidazole-1,3,4-oxadiazole derivatives (**5a–z**) have been synthesized and evaluated for their in vitro α-glucosidase and α-amylase inhibitory potentials and antioxidant properties. As a result of in vitro screening, compound **5g** was found to be the most effective-glucosidase inhibitor of the examined compounds (IC_{50}: 35.041.28 g/mL). The α-amylase inhibitory activity of the compound **5s** with an IC_{50}: 22.39 ± 1.49 µg/mL was found to be two times more effective than the reference drug acarbose (IC_{50}: 46.21±1.49 µg/mL). The results of the MTT cytotoxicity assay established the safety profile of active compounds **5o**, **5g**, **5s**, **5x**, and **5q**. In silico molecular docking study was performed to predict the interactions of all compounds with α-glucosidase and α-amylase. MD simulations study was performed for the confirmation of protein-ligand stability of compounds **5g** and **5q** with α-glucosidase, and compounds **5g**, **5s**, **5x**, and **5q** with α-amylase. Additionally, significant antioxidant qualities of components **5o**, **5g**, **5s**, **5x**, and **5q** may help to lessen difficulties caused by oxidative stress in people with diabetes.

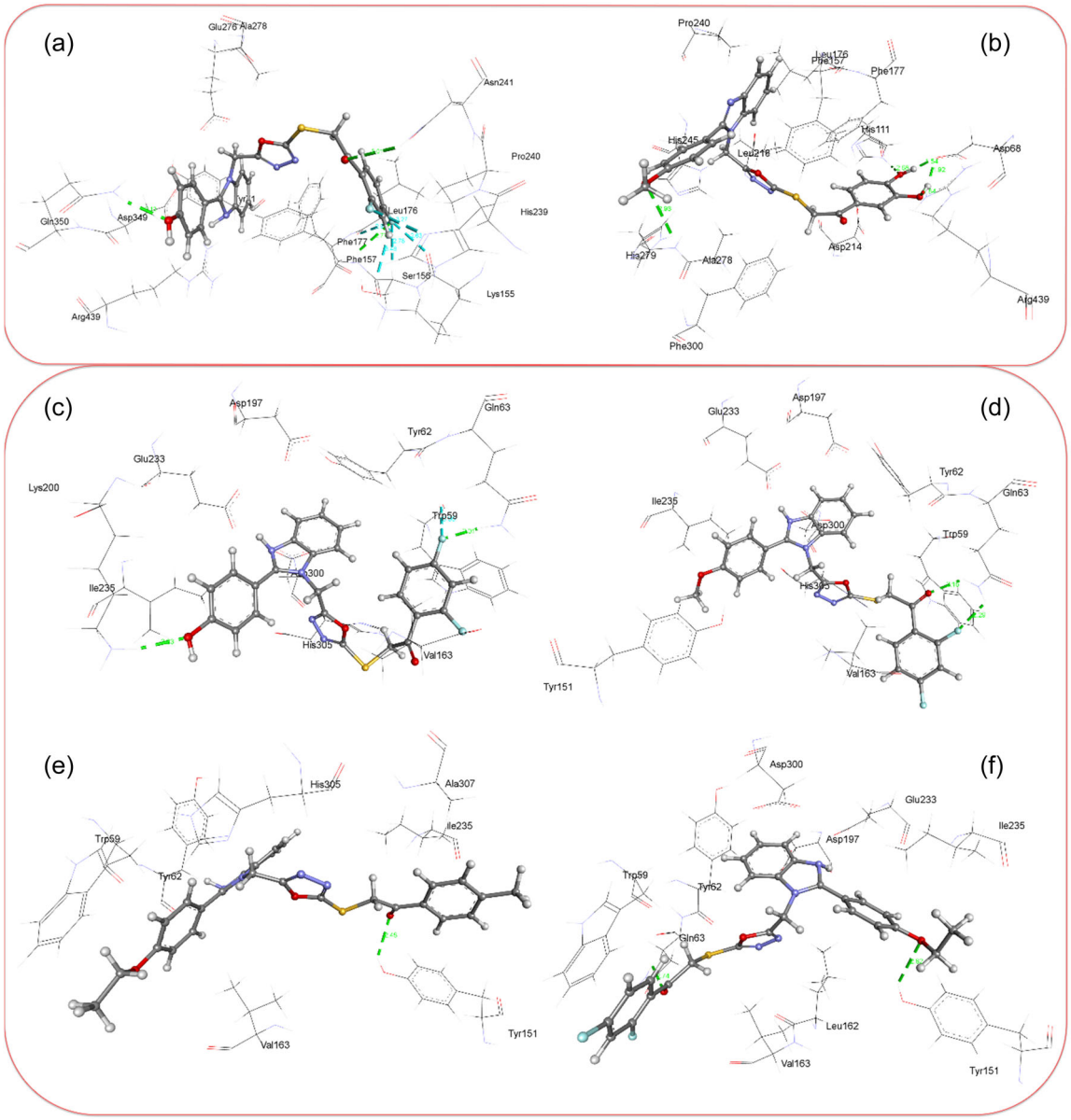

FIGURE 8 (a, b) Binding mode and interactions of compounds **5g** and **5q** at the α-glucosidase active site. (c–f) Binding pose of compounds **5g**, **5o**, **5s**, and **5x** at the α-amylase active pocket, respectively.

4 | EXPERIMENTAL

4.1 | Chemistry

4.1.1 | General

The whole chemicals used in the synthetic process were bought from Merck Chemicals or Sigma-Aldrich Chemicals (Sigma-Aldrich Corp.) (Merck KGaA). A Bruker digital FT NMR spectrometer (Bruker Bioscience) was used to record the ^{1}H and ^{13}C NMR spectra of the produced compounds in DMSO-d_6. Splitting patterns were designated as follows: s: singlet; d: doublet; t: triplet; m: multiplet in the NMR spectra. Hertz values for coupling constants (*J*) were given. Shimadzu LC/MS ITTOF equipment was used to determine M+1 peaks (Shimadzu). The uncorrected melting points of the resulting compounds were established using the MP90 digital melting point instrument (Mettler Toledo). Using Silica Gel 60 F254 TLC plates, thin-layer chromatography (TLC) was used to monitor each reaction (Merck KGaA).

The InChI codes of the investigated compounds, together with some biological activity data, are provided as Supporting Information.

4.1.2 | Synthesis of 2-(4-substitutedphenyl)-1*H*-benzimidazole derivatives (**1a–c**)

An Anton-Paar Monowave 300 was used to microwave irradiate a mixture of sodium metabisulfite (0.03 mol, 5.7 g) and 4-substituted

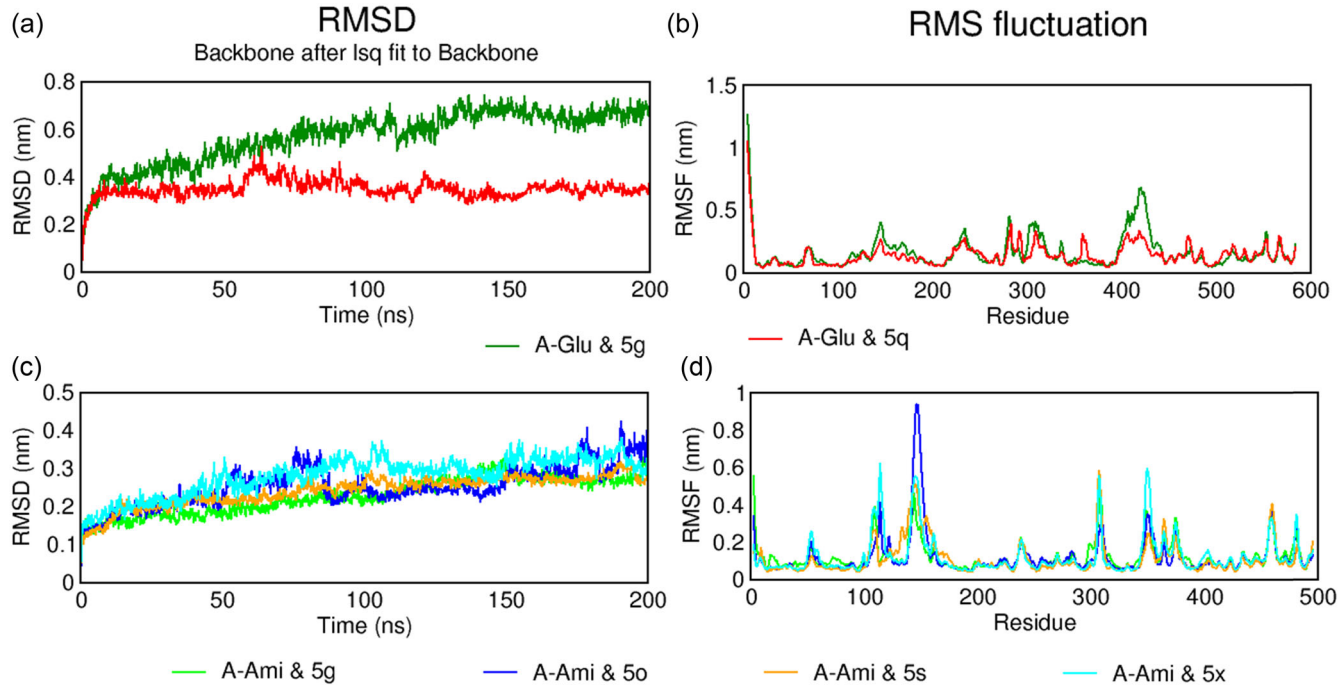

FIGURE 9 Root mean square deviation (RMSD), root mean square fluctuation (RMSF) results obtained from molecular dynamics simulation trajectory. (a, b) RMSD and RMSF graphs of α-glucosidase and **5g** (A-Glu and **5g**) and α-glucosidase and **5q** (A-Glu and **5q**) complexes. (c, d) α-amylase and **5g** (A-Ami and **5g**), α-amylase and **5o** (A-Ami and **5o**), α-amylase and **5s** (A-Ami and **5s**) and α-amylase and **5x** (A-Ami and **5x**) complexes for 200 ns.

benzaldehyde (0.03 mol, 240°C) for 5 min. *O*-Phenylenediamine (0.03 mol) was added after the mixture had cooled and held under the same reaction conditions. The combination was put onto crushed ice after the reaction was finished. The resulting solid was filtered, water-washed, dried, and then recrystallized from ethanol.

4.1.3 | Synthesis of ethyl 2-[2-(4-substitutedphenyl)-1*H*-benzimidazole-1-yl]acetate derivatives (**2a–c**)

2-(4-Substitutedphenyl)-1*H*-benzimidazole derivatives (**1a–c**) derivative compound (0.025 mol) and chloroethylacetate were dissolved in THF and NaH were added into the mixture. The reaction mixture was refluxed. After TLC control, the solvent was evaporated. The residue was dried, then recrystallized from ethanol after being rinsed with water.

4.1.4 | Synthesis of 2-[2-(4-substitutedphenyl)-1*H*-benzimidazole-1yl]acetohydrazide derivatives (**3a–c**)

Ethyl 2-[2-(4-substitutedphenyl)-1*H*-benzimidazole-1-yl]acetate (0.018 mol) and excess of hydrazine hydrate (5 mL) in ethanol (15 mL) were mixed in a vial (30 mL) of microwave synthesis reactor (Anton-Paar Monowave 300). For 10 min, the reaction mixture was heated at 80°C and 10 bar. The product was then filtered, water-washed, dried, and recrystallized from ethanol once the mixture had cooled.

4.1.5 | Synthesis of 5-{[2-(4-substitutedphenyl)-1*H*-benzimidazole-1-yl]-methyl}-1,3,4-oxadiazol-2-yl (**4a–c**)

2-[2-(4-Substitutedphenyl)-1*H*-benzimidazole-1yl]acetohydrazide derivatives (**3a–c**) (0.01 mol) was dissolved in a solution of NaOH (0.01 mol, 0.4 g) in ethanol and carbon disulfide (0.01 mol, 0.60 mL) was added in the mixture. For 8 h, the mixture was refluxed. After the reaction was complete, the solution was cooled and the desired chemical was obtained by acidifying it to a pH of 4–5 using strong hydrochloric acid solution.

4.1.6 | Synthesis of 2-[(5-{[2-(4-substitutedphenyl)-1*H*-benzimidazole-1-yl]methyl}-1,3,4-oxadiazol-2-yl) thio]-1-(substitutedphenyl)ethan-1-one (**5a–z**)

5-{[2-(4-Substitutedphenyl)-1*H*-benzimidazole-1-yl]-methyl}-1,3,4-oxadiazol-2-yl (**4a–c**) (0.001 mol), potassium carbonate (0.001 mol, 0.138 g) and substituted phenacyl bromide (0.0015 mol) derivative were dissolved in acetone and refluxed for 6 h. The solvent was evaporated after TLC control, the residue was washed with water,

dried, and then recrystallized from ethanol to produce the final products (**5a–z**).

*2-[(5-{[2-(4-Hydroxyphenyl)-1H-benzimidazole-1-yl)methyl}-1,3,4-oxadiazol-2-yl)thio]-1-phenylethan-1-one (**5a**)*

Yield: 72%, M.p.: 125.3–126.8°C. ^{1}H NMR (300 MHz, DMSO-d_6, 36°C, TMS): δ 12.89 (s,1H, OH), 8.16–8.12 (m, 3H, Aromatic CH), 8.06–8.03 (m, 2H, Aromatic CH), 7.70–7.67 (m, 2H, Aromatic CH), 7.60–7.54 (m, 3H, Aromatic CH), 7.24–7.20 (m, 3H, Aromatic CH), 5.49 (s, 2H, CH_2), 5.14 (s, 2H, CH_2). ^{13}C NMR (75 MHz, DMSO-d_6, 36°C, TMS): δ = 193.13 (C═O), 167.20, 163.98, 143.64, 134.50, 129.38, 128.93, 128.52, 126.80, 125.05, 123.97, 122.62, 115.71, 114.01, 113.05, 111.85, 111.53, 110.41, 60.89 (CH_2), 59.64 (CH_2). HRMS (*m/z*): $[M+H]^+$ calcd for $C_{24}H_{18}N_4O_3S$: 443.1158; found: 443.1172.

*2-[(5-{[2-(4-Hydroxyphenyl)-1H-benzimidazole-1-yl)methyl}-1,3,4-oxadiazol-2-yl)thio]-1-(4-tolyl)ethan-1-one (**5b**)*

Yield: 77%, M.p.: 124.4–126.1°C. ^{1}H NMR (300 MHz, DMSO-d_6, 36°C, TMS): δ 12.85 (s, 1H, OH), 8.12 (d, *J* = 8.55 Hz, 2H, 1,4-disubstitutedbenzene), 7.92 (d, *J* = 8.25 Hz, 2H, 1,4-disubstitute-dbenzene), 7.36 (d, *J* = 7.92 Hz, 2H, 1,4-disubstitutedbenzene), 7.24–7.21 (m, 3H, Aromatic CH), 7.19–7.16 (m, 3H, Aromatic CH), 5.49 (s, 2H, CH_2), 5.11 (s, 2H, CH_2), 2.37 (s, 3H, CH_3). ^{13}C NMR (75 MHz, DMSO-d_6, 36°C, TMS): δ = 192.21 (C═O), 165.05, 163.90, 158.88, 151.47, 145.07, 132.91, 129.89, 129.03, 128.50, 125.90, 124.38, 123.83, 122.65, 121.99, 115.72, 115.60, 111.90, 60.52 (CH_2), 59.87 (CH_2), 21.67 (CH_3). HRMS (*m/z*): $[M+H]^+$ calcd for $C_{25}H_{20}N_4O_3S$: 457.1320; found: 457.1329.

*2-[(5-{[2-(4-Hydroxyphenyl)-1H-benzimidazole-1-yl)methyl}-1,3,4-oxadiazol-2-yl)thio]-1-(4-chlorophenyl)ethan-1-one (**5c**)*

Yield: 74%, M.p.: 121.4–123.7°C. ^{1}H NMR (300 MHz, DMSO-d_6, 36°C, TMS): δ 8.15 (d, *J* = 8.40 Hz, 2H, 1,4-disubstitutedbenzene), 8.06 (d, *J* = 8.79 Hz, 2H, 1,4-disubstitutedbenzene), 7.66–7.63 (m, 3H, Aromatic CH), 7.61–7.59 (m, 2H, Aromatic CH), 7.27–7.20 (m, 3H, Aromatic CH), 5.51 (s, 2H, CH_2), 5.14 (s, 2H, CH_2). ^{13}C NMR (75 MHz, DMSO-d_6, 36°C, TMS): δ = 191.91 (C═O), 164.92, 163.94, 159.11, 151.23, 143.29, 139.41, 138.11, 134.13, 131.98, 130.85, 129.50, 128.70, 123.49, 122.70, 117.65, 115.78, 114.47, 60.17 (CH_2), 59.90 (CH_2). HRMS (*m/z*): $[M+H]^+$ calcd for $C_{24}H_{17}N_4O_3SCl$: 477.0764; found: 477.0783.

*2-[(5-{[2-(4-Hydroxyphenyl)-1H-benzimidazole-1-yl)methyl}-1,3,4-oxadiazol-2-yl)thio]-1-(4-fluorophenyl)ethan-1-one (**5d**)*

Yield: 68%, M.p.: 119.1–121.2°C. ^{1}H NMR (300 MHz, DMSO-d_6, 36°C, TMS): δ = 12.90 (s, 1H, OH), 8.16-8.13 (m, 3H, Aromatic CH), 8.11 (s, 1H, Aromatic CH), 7.44–7.38 (m, 2H, Aromatic CH), 7.24–7.21 (m, 3H, Aromatic CH), 7.20–7.16 (m, 3H, Aromatic CH), 5.50 (s, 2H, CH_2), 5.15 (s, 2H, CH_2). ^{13}C NMR (75 MHz, DMSO-d_6, 36°C, TMS): δ = 191.42 (C═O), 163.95, 159.28, 148.37, 138.71, 136.22, 132.12, 131.99, 131.54, 128.52, 124.36, 122.33, 116.61, 116.32, 115.70, 114.19, 106.60, 104.84, 60.68 (CH_2), 59.54 (CH_2). HRMS (*m/z*): $[M+H]^+$ calcd for $C_{24}H_{17}N_4O_3FS$: 461.1061; found: 461.1078.

*2-[(5-{[2-(4-Hydroxyphenyl)-1H-benzimidazole-1-yl)methyl}-1,3,4-oxadiazol-2-yl)thio]-1-(4-bromophenyl)ethan-1-one (**5e**)*

Yield: 72%, M.p.:119.2–120.8°C. ^{1}H NMR (300 MHz, DMSO-d_6, 36°C, TMS): δ = 12.85 (s, 1H, OH), 8.14 (d, *J* = 6.84 Hz, 2H, 1,4-disubstitutedbenzene), 8.11–8.10 (m, 2H, Aromatic CH), 7.97 (d, *J* = 8.61 Hz, 2H, 1,4-disubstitutedbenzene), 7.78 (d, *J* = 8.61 Hz, 2H, 1,4-disubstitutedbenzene), 7.22 (d, *J* = 6.90 Hz, 2H, 1,4-disubstitutedbenzene), 7.18–7.16 (m, 2H, Aromatic CH), 5.49 (s, 2H, CH_2), 5.13 (s, 2H, CH_2). ^{13}C NMR (75 MHz, DMSO-d_6, 36°C, TMS): δ = 192.64 (C═O), 159.39, 150.97, 145.15, 135.95, 134.46, 132.66, 131.85, 130.90, 129.44, 128.51, 127.27, 124.68, 122.09, 117.41, 115.59, 112.11, 110.55, 60.47 (CH_2), 56.10 (CH_2). HRMS (*m/z*): $[M+H]^+$ calcd for $C_{24}H_{17}N_4O_3SBr$: 521.0272; found: 521.0277.

*2-[(5-{[2-(4-Hydroxyphenyl)-1H-benzimidazole-1-yl)methyl}-1,3,4-oxadiazol-2-yl)thio]-1-(4-cyanophenyl)ethan-1-one (**5f**)*

Yield: 69%, M.p.: 130.4–132.2°C. ^{1}H NMR (300 MHz, DMSO-d_6, 36°C, TMS): δ = 8.17 (d, *J* = 8.67 Hz, 2H, 1,4-disubstitutedbenzene), 8.13–8.11 (m, 2H, Aromatic CH), 8.05 (d, *J* = 8.55 Hz, 2H, 1,4-disubstitutedbenzene), 7.58–7.56 (m, 2H, Aromatic CH), 7.26–7.24 (m, 2H, Aromatic CH), 7.21–7.20 (m, 2H, Aromatic CH), 5.49 (s, 2H, CH_2), 5.17 (s, 2H, CH_2). ^{13}C NMR (75 MHz, DMSO-d_6, 36°C, TMS): δ = 191.60 (C═O), 171.34, 168.01, 157.31, 151.80, 144.77, 137.23, 133.39, 131.33, 129.51, 128.64, 126.14, 124.27, 122.64, 119.07, 115.77, 113.67, 110.86, 108.58, 60.26 (CH_2), 54.96 (CH_2). HRMS (*m/z*): [M+H] calcd for $C_{25}H_{17}N_5O_3S$: 468.1114; found: 468.1125.

*2-[(5-{[2-(4-Hydroxyphenyl)-1H-benzimidazole-1-yl)methyl}-1,3,4-oxadiazol-2-yl)thio]-1-(2,4-difluorophenyl)ethan-1-one (**5g**)*

Yield: 72%, M.p.: 164.1–166.1°C. ^{1}H NMR (300 MHz, DMSO-d_6, 36°C, TMS): δ = 8.16 (d, *J* = 8.91 Hz, 2H, 1,4-disubstitutedbenzene), 7.61–7.58 (m, 3H, Aromatic CH), 7.25 (d, *J* = 8.94 Hz, 2H, 1,4-disubstitutedbenzene), 7.22–7.20 (m, 4H, Aromatic CH), 5.51 (s, 2H, CH_2), 5.39 (s, 2H, CH_2). ^{13}C NMR (75 MHz, DMSO-d_6, 36°C, TMS): δ = 191.39 (C═O), 178.59, 159.84, 159.05, 151.25, 145.10142.07, 139.19, 138.57, 128.69, 123.81, 123.62, 123.23, 122.68, 116.31, 115.80, 115.47, 115.33, 115.25, 115.13, 60.10 (CH_2), 58.19 (CH_2). HRMS (*m/z*): [M+H] calcd for $C_{24}H_{16}N_4O_3F_2S$: 479.0969; found: 479.0984.

*2-[(5-{[2-(4-Hydroxyphenyl)-1H-benzimidazole-1-yl)methyl}-1,3,4-oxadiazol-2-yl)thio]-1-(2,4-dichlorophenyl)ethan-1-one (**5h**)*

Yield: 77%, M.p.: 178.2–179.4°C. ^{1}H NMR (300 MHz, DMSO-d_6, 36°C, TMS): δ = 8.17–8.16 (m, 2H, Aromatic CH), 7.92–7.88 (m, 2H, Aromatic CH), 7.63–7.62 (m, 1H, Aromatic CH), 7.58–7.56 (m, 3H, Aromatic CH), 7.20–7.19 (m, 3H, Aromatic CH), 5.49 (s, 2H, CH_2), 4.98 (s, 2H, CH_2). ^{13}C NMR (75 MHz, DMSO-d_6, 36°C, TMS): δ = 193.47 (C═O), 164.32, 160.32, 158.66, 151.59, 143.39, 137.15, 132.28, 131.74, 131.57, 131.10, 128.80, 128.61, 128.42, 122.67, 122.60, 116.15, 115.97, 115.71, 110.66, 60.16 (CH_2), 58.60 (CH_2). HRMS (*m/z*): $[M+H]^+$ calcd for $C_{24}H_{16}N_4O_3SCl_2$: 511.0379; found: 511.0393.

*2-[(5-{[2-(4-Hydroxyphenyl)-1H-benzimidazole-1-yl)methyl}-1,3,4-oxadiazol-2-yl)thio]-1-(3,4-dihydroxyphenyl)ethan-1-one (**5i**)*

Yield: 66%, M.p.: 178.6–180.1°C. ^{1}H NMR (300 MHz, DMSO-d_6, 36°C, TMS): δ = 8.15 (d, J = 8.79 Hz, 2H, 1,4-disubstitutedbenzene). 7.45–7.41 (m, 1H, Aromatic CH), 7.37 (s, 1H, Aromatic CH), 7.22 (d, J = 8.85 Hz, 2H, 1,4-disubstitutedbenzene), 7.18–7.15 (m, 2H, Aromatic CH), 6.80 (d, J = 7.95 Hz, 1H, Aromatic CH), 5.48 (s, 2H, CH_2), 5.01 (s, 2H, CH_2). ^{13}C NMR (75 MHz, DMSO-d_6, 36°C, TMS): δ = 190.57 (C═O), 165.29, 163.79, 158.89, 152.61, 151.48, 149.39, 145.99, 139.80, 137.34, 135.54, 134.08, 128.54, 126.80, 124.38, 122.60, 122.31, 118.86, 117.41, 115.71, 59.91 (CH_2), 54.55 (CH_2). HRMS (*m/z*): $[M+H]^+$ calcd for $C_{24}H_{18}N_4O_5S$: 475.1062; found: 475.1071.

*2-[(5-{[2-(4-Methoxyphenyl)-1H-benzimidazole-1-yl)methyl}-1,3,4-oxadiazol-2-yl)thio]-1-(4-tolyl)ethan-1-one (**5j**)*

Yield: 69%, M.p.: 94.2–96.3°C. ^{1}H NMR (300 MHz, DMSO-d_6, 36°C, TMS): δ = 7.93 (d, J = 8.31 Hz, 2H, 1,4-disubstitutedbenzene), 7.79 (d, J = 8.79 Hz, 2H, 1,4-disubstitutedbenzene), 7.72–7.71 (m, 2H, Aromatic CH), 7.37 (d, J = 8.37 Hz, 2H, 1,4-disubstitutedbenzene), 7.30–7.27 (m, 2H, Aromatic CH), 7.14 (d, J = 8.94 Hz, 2H, 1,4-disubstitutedbenzene), 5.58 (s, 2H, CH_2), 5.05 (s, 2H, CH_2), 3.86 (s, 3H, OCH_3), 2.39 (s, 3H, CH_3). ^{13}C NMR (75 MHz, DMSO-d_6, 36°C, TMS): δ = 192.65 (C═O), 179.70, 163.79, 161.00, 159.13, 153.44, 144.92, 142.91, 136.21, 133.08, 131.23, 129.86, 129.06, 122.86, 122.12, 119.44, 114.77, 111.34, 60.14 (OCH_3), 55.83 (CH_2), 42.16 (CH_2), 21.69 (CH_3). HRMS (*m/z*): [M+H] calcd for $C_{26}H_{22}N_4O_3S$: 471.1467; found: 471.1485.

*2-[(5-{[2-(4-Methoxyphenyl)-1H-benzimidazole-1-yl)methyl}-1,3,4-oxadiazol-2-yl)thio]-1-(4-chlorophenyl)ethan-1-one (**5k**)*

Yield: 76%, M.p.: 93.6–95.2°C. ^{1}H NMR (300 MHz, DMSO-d_6, 36°C, TMS): δ = 7.96–7.92 (m, 1H, Aromatic CH), 7.83 (d, J = 8.88 Hz, 2H, 1,4-disubstitutedbenzene), 7.76 (d, J = 8.64 Hz, 1H, Aromatic CH), 7.66–7.65 (m, 2H, Aromatic CH), 7.57–7.56 (m, 2H, Aromatic CH), 7.28–7.24 (m, 2H, Aromatic CH), 7.14 (d, J = 8.88 Hz, 2H, 1,4-disubstitutedbenzene), 5.45 (s, 2H, CH_2), 5.06 (s, 2H, CH_2), 3.86 (s, 3H, OCH_3). ^{13}C NMR (75 MHz, DMSO-d_6, 36°C, TMS): δ = 191.91 (C═O), 158.66, 142.93, 142.54, 136.27, 135.67, 131.48, 131.25, 130.86, 129.49, 129.00, 128.48, 122.89, 122.71, 122.30, 119.36, 114.73, 111.44, 59.73 (OCH_3), 55.87 (CH_2), 42.09 (CH_2). HRMS (*m/z*): $[M+H]^+$ calcd for $C_{25}H_{19}N_4O_3SCl$: 491.0932; found: 491.0939.

*2-[(5-{[2-(4-Methoxyphenyl)-1H-benzimidazole-1-yl)methyl}-1,3,4-oxadiazol-2-yl)thio]-1-(4-fluorophenyl)ethan-1-one (**5l**)*

Yield: 78%, M.p.: 100.1–101.6°C. ^{1}H NMR (300 MHz, DMSO-d_6, 36°C, TMS): δ = 8.15–8.12 (m, 1H, Aromatic CH), 7.91–7.88 (m, 2H, Aromatic CH), 7.81 (d, J = 8.85 Hz, 2H, Aromatic CH), 7.68–7.66 (m, 1H, Aromatic CH), 7.59–7.56 (m, 1H, Aromatic CH), 7.29–7.24 (m, 3H, Aromatic CH), 7.13 (d, J = 8.88 Hz, 2H, 1,4-disubstitutedbenzene), 5.81 (s, 2H, CH_2), 5.44 (s, 2H, CH_2), 3.85 (s, 3H, OCH_3). ^{13}C NMR (75 MHz, DMSO-d_6, 36°C, TMS): δ = 192.43 (C═O), 160.96, 158.66, 153.37, 142.93, 136.26, 132.23, 131.85, 131.25, 128.49, 122.90, 122.71, 122.30, 119.36, 116.45, 115.70, 114.73, 114.32, 111.42, 60.37 (OCH_3), 55.83 (CH_2), 46.34 (CH_2). HRMS (*m/z*): $[M+H]^+$ calcd for $C_{25}H_{19}N_4O_3FS$: 475.1211; found: 475.1235.

*2-[(5-{[2-(4-Methoxyphenyl)-1H-benzimidazole-1-yl)methyl}-1,3,4-oxadiazol-2-yl)thio]-1-(4-bromophenyl)ethan-1-one (**5m**)*

Yield: 66%, M.p.: 100.5–101.7°C. ^{1}H NMR (300 MHz, DMSO-d_6, 36°C, TMS): δ = 8.15–8.12 (m, 1H, Aromatic CH), 7.82 (d, J = 8.79 Hz, 2H, Aromatic CH), 7.75–7.73 (m, 2H, Aromatic CH), 7.71–7.70 (m, 2H, Aromatic CH), 7.28–7.27 (m, 3H, Aromatic CH), 7.15 (d, J = 8.85 Hz, 2H, 1,4-disubstitutedbenzene), 5.78 (s, 2H, CH_2), 5.47 (s, 2H, CH_2), 3.86 (s, 3H, OCH_3). ^{13}C NMR (75 MHz, DMSO-d_6, 36°C, TMS): δ = 191.37 (C═O), 160.95, 158.67, 153.37, 142.93, 136.26, 132.45, 132.13, 131.36, 131.25, 128.47, 123.20, 122.90, 122.72, 122.29, 119.36, 114.74, 111.42, 58.86 (OCH_3), 55.83 (CH_2), 41.63 (CH_2). HRMS (*m/z*): $[M+H]^+$ calcd for $C_{25}H_{19}N_4O_3SBr$: 535.0421; found: 535.0434.

*2-[(5-{[2-(4-Methoxyphenyl)-1H-benzimidazole-1-yl)methyl}-1,3,4-oxadiazol-2-yl)thio]-1-(4-cyanophenyl)ethan-1-one (**5n**)*

Yield: 62%, M.p.: 104.2–105.9°C. ^{1}H NMR (300 MHz, DMSO-d_6, 36°C, TMS): δ = 8.12–8.11 (m, 2H, Aromatic CH), 7.97–7.94 (m, 2H, Aromatic CH), 7.83 (d, J = 8.88 Hz, 2H, Aromatic CH), 7.67–7.66 (m, 1H, Aromatic CH), 7.27–7.25 (m, 3H, Aromatic CH), 7.15 (d, J = 8.88 Hz, 2H, 1,4-disubstitutedbenzene), 5.77 (s, 2H, CH_2), 5.45 (s, 2H, CH_2), 3.86 (s, 3H, OCH_3). ^{13}C NMR (75 MHz, DMSO-d_6, 36°C, TMS): δ = 197.73 (C═O), 161.26, 158.67, 153.36, 142.94, 136.35, 133.33, 132.99, 131.25, 130.34, 123.71, 122.89, 122.71, 122.30, 120.87, 119.61, 119.36, 114.73, 111.42, 59.29 (OCH_3), 55.83 (CH_2), 43.16 (CH_3). HRMS (*m/z*): [M+H] calcd for $C_{26}H_{19}N_5O_3S$: 482.1271; found: 482.1281.

*2-[(5-{[2-(4-Methoxyphenyl)-1H-benzimidazole-1-yl)methyl}-1,3,4-oxadiazol-2-yl)thio]-1-(2,4-difluorophenyl)ethan-1-one (**5o**)*

Yield: 70%, M.p.: 105.3–106.4°C. ^{1}H NMR (300 MHz, DMSO-d_6, 36°C, TMS): δ = 7.81 (d, J = 8.82 Hz, 2H, 1,4-disubstitutedbenzene), 7.75–7.72 (m, 2H, Aromatic CH), 7.68–7.65 (m, 2H, Aromatic CH), 7.27–7.25 (m, 3H, Aromatic CH), 7.13 (d, J = 8.91 Hz, 2H, 1,4-disubstitutedbenzene), 5.78 (s, 2H, CH_2), 5.44 (s, 2H, CH_2), 3.85 (s, 3H, OCH_3). ^{13}C NMR (75 MHz, DMSO-d_6, 36°C, TMS): δ = 190.28 (C═O), 165.34, 143.75, 143.11, 138.64, 138.20, 131.25, 130.83, 130.05, 125.33, 123.70, 123.09, 119.42, 118.47, 115.99, 115.82, 114.73, 113.72, 110.17, 106.72, 55.86 (OCH_3), 54.84 (CH_2), 42.95 (CH_2). HRMS (*m/z*): [M+H] calcd for $C_{25}H_{18}N_4O_3F_2S$: 493.1120; found: 493.1140.

*2-[(5-{[2-(4-Methoxyphenyl)-1H-benzimidazole-1-yl)methyl}-1,3,4-oxadiazol-2-yl)thio]-1-(2,4-dichlorophenyl)ethan-1-one (**5p**)*

Yield: 73%, M.p.: 129.5–130.4°C. ^{1}H NMR (300 MHz, DMSO-d_6, 36°C, TMS): δ = 7.76 (d, J = 8.82 Hz, 2H, 1,4-disubstitutedbenzene), 7.70–7.67 (m, 2H, Aromatic CH), 7.63–7.60 (m, 1H, Aromatic CH), 7.56–7.54 (1H, m, Aromatic CH), 7.29–7.27 (m, 3H, Aromatic CH), 7.13 (d, J = 8.91 Hz, 2H, 1,4-disubstitutedbenzene), 5.81 (s, 2H, CH_2), 5.61

(s, 2H, CH_2), 3.85 (s, 3H, OCH_3). ^{13}C NMR (75 MHz, DMSO-d_6, 36°C, TMS): δ = 191.49 (C=O), 161.04, 159.54, 158.23, 153.50, 143.09, 136.17, 133.32, 132.91, 131.22, 130.36, 128.54, 128.06, 123.22, 122.99, 122.34, 121.97, 119.51, 114.79, 111.27, 57.98 (OCH_3), 55.84 (CH_2), 48.59 (CH_2). HRMS (*m/z*): $[M+H]^+$ calcd for $C_{25}H_{18}N_4O_3SCl_2$: 525.0554; found: 525.0549.

*2-[(5-{[2-(4-Methoxyphenyl)-1*H*-benzimidazole-1-yl)methyl}-1,3,4-oxadiazol-2-yl)thio]-1-(3,4-dihydroxyphenyl)ethan-1-one (**5q**)*

Yield: 65%, M.p.: 227.6–229.3°C. ^{1}H NMR (300 MHz, DMSO-d_6, 36°C, TMS): δ = 7.73 (d, *J* = 8.85 Hz, 2H, 1,4-disubstitutedbenzene), 7.62–7.59 (m, 1H, Aromatic CH), 7.42–7.34 (m, 3H, Aromatic CH), 7.29–7.26 (m, 2H, Aromatic CH), 7.10 (d, *J* = 8.88 Hz, 2H, 1,4-disubstitutedbenzene), 6.81 (d, *J* = 8.28 Hz, 1H, 1,4-disubstitutedbenzene), 5.77 (s, 2H, CH_2), 4.94 (s, 2H, CH_2), 3.83 (s, 3H, OCH_3). ^{13}C NMR (75 MHz, DMSO-d_6, 36°C, TMS): δ = 189.88 (C=O), 165.03, 163.66, 161.02, 153.54, 146.48, 142.93, 136.11, 131.20, 128.46, 124.99, 123.22, 123.12, 122.99, 121.99, 119.55, 115.35, 114.78, 114.32, 111.18, 57.59 (OCH_3), 55.78 (CH_2), 42.27 (CH_2). HRMS (*m/z*): $[M+H]^+$ calcd for $C_{25}H_{20}N_4O_5S$: 489.1213; found: 489.1227.

*2-[(5-{[2-(4-Ethoxyphenyl)-1*H*-benzimidazole-1-yl)methyl}-1,3,4-oxadiazol-2-yl)thio]-1-phenylethan-1-one (**5r**)*

Yield: 66%, M.p.: 189.1–190.6°C. ^{1}H NMR (300 MHz, DMSO-d_6, 36°C, TMS): δ = 8.11 (d, *J* = 8.73 Hz, 1H, Aromatic CH), 7.76 (d, *J* = 8.82 Hz, 2H, Aromatic CH), 7.69–7.67 (m, 2H, Aromatic CH), 7.62–7.59 (m, 3H, Aromatic CH), 7.29–7.26 (m, 3H, Aromatic CH), 7.11 (d, *J* = 8.76 Hz, 2H, Aromatic CH), 5.77 (s, 2H, CH_2), 5.57 (s, 2H, CH_2), 4.17–4.12 (m, 2H, CH_2), 1.37 (t, *J* = 6.93 Hz, 3H, CH_3). ^{13}C NMR (75 MHz, DMSO-d_6, 36°C, TMS): δ = 191.80 (C=O), 160.30, 159.17, 153.47, 142.91, 136.21, 131.23, 129.72, 129.38, 129.04, 128.49, 123.06, 122.85, 122.22, 121.95, 119.44, 115.14, 111.32, 63.77 (CH_2), 56.83 (CH_2), 44.87 (CH_2), 15.07 (CH_3). HRMS (*m/z*): $[M+H]^+$ calcd for $C_{26}H_{22}N_4O_3S$: 471.1463; found: 471.1485.

*2-[(5-{[2-(4-Ethoxyphenyl)-1*H*-benzimidazole-1-yl)methyl}-1,3,4-oxadiazol-2-yl)thio]-1-(4-tolyl)ethan-1-one (**5s**)*

Yield: 64%, M.p.: 148.5–149.7°C. ^{1}H NMR (300 MHz, DMSO-d_6, 36°C, TMS): δ = 7.91–7.88 (m, 1H, Aromatic CH), 7.76–7.70 (m, 3H, Aromatic CH), 7.62–7.53 (m, 2H, Aromatic CH), 7.38–7.35 (m, 1H, Aromatic CH), 7.29–7.25 (m, 2H, Aromatic CH), 7.18–7.16 (m, 1H, Aromatic CH), 7.13–7.04 (m, 2H, Aromatic CH), 5.76 (s, 2H, CH_2), 5.60 (2H, s, CH_2), 4.13–4.10 (m, 2H, CH_2), 2.39 (s, 3H, CH_3), 1.37 (t, *J* = 6.51 Hz, 3H, CH_3). ^{13}C NMR (75 MHz, DMSO-d_6, 36°C, TMS): δ = 192.22 (C=O), 163.79, 160.31, 153.54, 145.08, 131.19, 129.89, 129.60, 129.01, 128.53, 123.19, 122.95, 122.29, 121.81, 119.54, 115.15, 111.27, 111.15, 63.75 (CH_2), 61.18 (CH_2), 44.21 (CH_2), 21.72 (OCH_3), 15.07 (OCH_3). HRMS (*m/z*): $[M+H]^+$ calcd for $C_{27}H_{24}N_4O_3S$: 485.1622; found: 485.1642.

*2-[(5-{[2-(4-Ethoxyphenyl)-1*H*-benzimidazole-1-yl)methyl}-1,3,4-oxadiazol-2-yl)thio]-1-(4-chlorophenyl)ethan-1-one (**5t**)*

Yield: 71%, M.p.: 187.9–189.3°C. ^{1}H NMR (300 MHz, DMSO-d_6, 36°C, TMS): δ = 8.14–8.11 (m, 1H, Aromatic CH), 8.02–7.99 (m, 1H, Aromatic CH), 7.73–7.66 (m, 2H, Aromatic CH), 7.63–7.62 (m, 2H, Aromatic CH), 7.30–7.28 (m, 3H, Aromatic CH), 7.13–7.08 (m, 3H, Aromatic CH), 5.78 (s, 2H, CH_2), 5.64 (s, 2H, CH_2), 4.15–4.09 (m, 2H, CH_2), 2.39 (s, 3H, CH_3), 1.37 (t, *J* = 6.87 Hz, 3H, CH_3). ^{13}C NMR (75 MHz, DMSO-d_6, 36°C, TMS): δ= 191.49 (C=O), 163.86, 159.54, 153.52, 142.87, 136.17, 134.08, 131.21, 130.80, 129.48, 128.59, 123.20, 122.99, 122.37, 121.80, 119.51, 115.17, 111.25, 63.77 (CH_2), 61.09 (CH_2), 44.47 (CH_2), 15.07 (CH_3). HRMS (*m/z*): $[M+H]^+$ calcd for $C_{26}H_{21}N_4O_3SCl$: 505.1084; found: 505.1096.

*2-[(5-{[2-(4-Ethoxyphenyl)-1*H*-benzimidazole-1-yl)methyl}-1,3,4-oxadiazol-2-yl)thio]-1-(4-fluorophenyl)ethan-1-one (**5u**)*

Yield: 73%, M.p.: 181.8–182.9°C. ^{1}H NMR (300 MHz, DMSO-d_6, 36°C, TMS): δ = 8.18–8.13 (m, 2H, Aromatic CH), 8.03 (d, *J* = 8.40 Hz, 2H, Aromatic CH), 7.81–7.73 (m, 1H, Aromatic CH), 7.69–7.61 (m, 2H, Aromatic CH), 7.45–7.37 (m, 3H, Aromatic CH), 6.93 (d, *J* = 8.61 Hz, 2H, Aromatic CH), 5.64 (s, 2H, CH_2), 5.00 (s, 2H, CH_2), 4.07 (q, *J* = 6.75 Hz, 2H, CH_2), 1.25 (t, *J* = 6.84 Hz, 3H, CH_3). ^{13}C NMR (75 MHz, DMSO-d_6, 36°C, TMS): δ = 191.49 (C=O), 160.38, 159.73, 144.20, 142.79, 136.11, 133.00, 132.07, 131.22, 128.95, 123.31, 123.10, 119.49, 116.75, 116.60, 115.39, 115.19, 111.25, 63.77 (CH_2), 61.51 (CH_2), 43.85 (CH_2), 15.06 (CH_3). HRMS (*m/z*): $[M+H]^+$ calcd for $C_{26}H_{21}N_4O_3FS$: 489.1369; found: 489.1391.

*2-[(5-{[2-(4-Ethoxyphenyl)-1*H*-benzimidazole-1-yl)methyl}-1,3,4-oxadiazol-2-yl)thio]-1-(4-bromophenyl)ethan-1-one (**5v**)*

Yield: 77%, M.p.: 192.5–194.1°C. ^{1}H NMR (300 MHz, DMSO-d_6, 36°C, TMS): δ = 7.95–7.91 (m, 1H, Aromatic CH), 7.77–7.74 (m, 3H, Aromatic CH), 7.71–7.68 (m, 2H, Aromatic CH), 7.64–7.61 (m, 1H, Aromatic CH), 7.58–7.55 (m, 1H, Aromatic CH), 7.30–7.27 (m, 2H, Aromatic CH), 7.13–7.10 (m, 2H, Aromatic CH), 5.78 (s, 2H, CH_2), 5.61 (s, 2H, CH_2), 4.12 (q, *J* = 7.56 Hz, 2H, CH_2), 1.37 (t, *J* = 6.93 Hz, 3H, CH_3). ^{13}C NMR (75 MHz, DMSO-d_6, 36°C, TMS): δ = 192.52 (C=O), 179.18, 160.32, 159.37, 153.50, 142.89, 136.18, 132.43, 131.22, 130.86, 128.53, 123.14, 122.93, 122.27, 121.87, 119.48, 115.16, 114.14, 65.47 (CH_2), 63.77 (CH_2), 42.07 (CH_2), 15.07 (CH_3). HRMS (*m/z*): $[M+H]^+$ calcd for $C_{26}H_{21}N_4O_3SBr$: 549.0573; found: 549.0590.

*2-[(5-{[2-(4-Ethoxyphenyl)-1*H*-benzimidazole-1-yl)methyl}-1,3,4-oxadiazol-2-yl)thio]-1-(4-cyanophenyl)ethan-1-one (**5w**)*

Yield: 64%, M.p.: 183.1–184.5°C. ^{1}H NMR (300 MHz, DMSO-d_6, 36°C, TMS): δ = 8.08 (d, *J* = 8.43 Hz, 2H, Aromatic CH), 7.80 (d, *J* = 8.76 Hz, 2H, Aromatic CH), 7.78 (d, *J* = 8.79 Hz, 2H, Aromatic CH), 7.28–7.25 (m, 3H, Aromatic CH), 7.14–7.11 (m, 3H, Aromatic CH), 5.78 (s, 2H, CH_2), 5.48 (s, 2H, CH_2), 4.17–4.11 (m, 2H, CH_2), 1.37 (t, *J* = 6.96 Hz, 3H, CH_3). ^{13}C NMR (75 MHz, DMSO-d_6, 36°C, TMS): δ = 192.98 (C=O), 160.28, 158.98, 153.43, 142.91, 136.22, 133.17, 131.23, 130.40, 128.49, 127.73, 123.00, 122.80, 122.49, 122.20, 122.01, 119.41, 115.12, 111.35, 63.76 (CH_2), 60.92 (CH_2), 45.62 (CH_2), 15.08 (CH_3). HRMS (*m/z*): [M+H] calcd for $C_{27}H_{21}N_5O_3S$: 496.1437; found: 496.1438.

*2-[(5-{[2-(4-Ethoxyphenyl)-1H-benzimidazole-1-yl)methyl}-1,3,4-oxadiazol-2-yl)thio]-1-(2,4-difluorophenyl)ethan-1-one (**5x**)*

Yield: 70%, M.p.: 138.7–139.9°C. ^{1}H NMR (300 MHz, DMSO-d_6, 36°C, TMS): δ = 8.11 (d, J = 8.79 Hz, 1H, Aromatic CH), 7.80 (d, J = 8.76 Hz, 2H, Aromatic CH), 7.58–7.55 (m, 2H, Aromatic CH), 7.27–7.24 (m, 3H, Aromatic CH), 7.17–7.15 (m, 1H, Aromatic CH), 7.11 (d, J = 8.85 Hz, 2H, Aromatic CH), 5.78 (2H, s, CH_2), 5.44 (s, 2H, CH_2), 4.12 (q, J = 6.96 Hz, 2H, CH_2), 1.37 (t, J = 6.93 Hz, 3H, CH_3). ^{13}C NMR (75 MHz, DMSO-d_6, 36°C, TMS): δ = 190.94 (C=O), 160.32, 160.25, 158.67, 153.39, 142.93, 140.97, 140.10, 136.25, 132.91, 131.25, 125.74, 122.88, 122.71, 122.12, 119.35, 115.18, 115.10, 111.41, 63.76 (CH_2), 60.35 (CH_2), 44.82 (CH_2), 15.08 (CH_3). HRMS (*m/z*): [M+H] calcd for $C_{26}H_{20}N_4O_3F_2S$: 507.1281; found: 507.1297.

*2-[(5-{[2-(4-Ethoxyphenyl)-1H-benzimidazole-1-yl)methyl}-1,3,4-oxadiazol-2-yl)thio]-1-(2,4-dichlorophenyl)ethan-1-one (**5y**)*

Yield: 71%, M.p.: 166.5–168.0°C. ^{1}H NMR (300 MHz, DMSO-d_6, 36°C, TMS): δ = 7.70 (d, J = 8.85 Hz, 2H, 1,4-disubstitutedbenzene), 7.61–7.58 (m, 1H, Aromatic CH), 7.43–7.36 (m, 2H, Aromatic CH), 7.28–7.25 (m, 2H, Aromatic CH), 7.07 (d, J = 8.82 Hz, 2H, 1,4-disubstitutedbenzene), 6.83 (d, J = 8.25 Hz, 2H, 1,4-disubstitutedbenzene), 5.76 (s, 2H, CH_2), 4.95 (s, 2H, CH_2), 4.09 (q, J = 6.93 Hz, 2H, $-CH_2$), 1.37 (t, J = 6.93 Hz, 3H, $-CH_3$). ^{13}C NMR (75 MHz, DMSO-d_6, 36°C, TMS): δ = 190.53 (C=O), 164.92, 163.69, 160.31, 153.56, 152.49, 145.96, 142.93, 136.10, 131.19, 126.85, 123.20, 122.99, 122.60, 121.83, 119.56, 115.64, 115.43, 115.14, 111.17, 63.77 (CH_2), 55.11 (CH_2), 53.66 (CH_2), 15.07 (CH_3). HRMS (*m/z*): $[M+H]^+$ calcd for $C_{26}H_{20}N_4O_3SCl_2$: 539.0705; found: 539.0706.

*2-[(5-{[2-(4-Ethoxyphenyl)-1H-benzimidazole-1-yl)methyl}-1,3,4-oxadiazol-2-yl)thio]-1-(3,4-dihydroxyphenyl)ethan-1-one (**5z**)*

Yield: 67%, M.p.: 258.6–259.7°C. ^{1}H NMR (300 MHz, DMSO-d_6, 36°C, TMS): δ = 8.11 (d, J = 8.82 Hz, 2H, 1,4-disubstitutedbenzene), 7.70–7.66 (m, 1H, Aromatic CH), 7.58–7.54 (m, 2H, Aromatic CH), 7.30–7.24 (m, 1H, Aromatic CH), 7.18–7.15 (m, 3H, Aromatic CH), 7.08 (d, J = 8.91 Hz, 2H, 1,4-disubstitutedbenzene), 5.77 (s, 2H, CH_2), 5.46 (s, 2H, CH_2), 4.09 (q, J = 6.90 Hz, 2H, $-CH_2$), 1.37 (t, J = 6.96 Hz, 3H, $-CH_3$). ^{13}C NMR (75 MHz, DMSO-d_6, 36°C, TMS): δ = 190.56 (C=O), 160.32, 160.25, 151.82, 145.99, 142.94, 131.06, 128.49, 122.99, 122.70, 122.48, 122.30, 122.13, 121.85, 118.57, 115.19, 115.10, 111.40, 111.22, 63.72 (CH_2), 56.94 (CH_2), 55.07 (CH_2), 15.08 (CH_3). HRMS (*m/z*): $[M+H]^+$ calcd for $C_{26}H_{22}N_4O_5S$: 503.1395; found: 503.1384.

4.2 | Pharmacological/biological assays

4.2.1 | In vitro α-amylase and α-glucosidase inhibition assays

The method developed by Paşayeva et al. was applied in this investigation to measure the inhibitory activity of α-amylase and α-glucosidase.[53] The used concentrations of compounds ranged between 1 and 1000 µg/mL. The samples' absorbance was measured at 540 nm once the reaction came to an end. Acarbose served as the positive control in this investigation. The α-amylase inhibitory activity was calculated as Equation (1):

$$(\%) = \left[1 - \left(\frac{A_{\text{sample}}}{A_{\text{control}}}\right)\right] \times 100. \quad (1)$$

To determine the α-glucosidase inhibitory activity, the concentration of compounds was prepared between 1 and 1000 µg/mL. The increased absorbance at the end of the reaction caused by the released *p*-nitrophenol was measured at 400 nm in accordance with the procedure. Acarbose was employed as a positive control in this experiment. The calculation of the α-glucosidase inhibitory activity followed the instructions for the α-amylase method.

4.2.2 | Statistical analysis

The standard and experimental groups' values were compared using statistical analysis utilizing GraphPad Prism Software Version 8.0. The outcome is represented as the mean standard deviation (SD). The one-way analysis of variance with multiple comparison test was used to compare statistically significant values, and *p*-values of less than 0.05 were regarded as statistically significant.

4.2.3 | Antioxidant activity (total antioxidant status [TAS])

A commercial test produced by Rel Assay Diagnostics is used to determine the TAS. The sample's potential antioxidant structures are converted using this procedure from the dark blue-green ABTS radical form to the colorless reduced ABTS form. The total antioxidant capacity of the sample is determined by the change in absorbance at 660 nm. The reference material, which is an analog of vitamin E known as the Trolox equivalent, was utilized to calibrate the assay as the stable standard antioxidant solution. The kit method was followed when measuring TAS. The equation given below is computed in accordance with Equation (2) after determining the discrepancy between absorbance readings.[54]

$$\text{A2} - \text{A1} = \Delta\text{Abs} \quad \text{of} \quad \textit{standard} \quad \text{or} \quad \text{sample} \quad \text{or} \quad \text{H}_2\text{O},$$

$$\text{Results} = \frac{[\Delta\text{Abs} \quad \text{H}_2\text{O} - \Delta\text{Abs} \quad \text{Sample}]}{[\Delta\text{Abs} \quad \text{H}_2\text{O} - \Delta\text{Abs} \quad \textit{Standard}]}. \quad (2)$$

4.2.4 | Cytotoxicity assay

The cytotoxicity assay of compounds **5a–z** was determined by the absorbance values obtained from MTT assays. The MTT method

was performed as previously described.[55] L929 healthy mouse fibroblast cells were used to evaluate the cytotoxicity of the compounds.

4.3 | Molecular docking

The Maestro graphical user interface of the Schrodinger 2022.2 version was used for the molecular docking experiment. It was selected from PDB for the target enzymes α-glucosidase (PDB ID: 5NN8)[56–58] and α-amylase (PDB ID: 1OSE).[57–59] Using the AlphaFold[58,59] protein structure database, incomplete residues in the 5NN8 structure were filled in. Both of the target proteins' structures were created using the default settings of the "Protein Preparation Wizard" in OPLS4 force fields. ChemDraw Professional 17.0 was used to create their composite structures, which were then reduced using OPLS4 force fields using "LigPrep" and "Epik" at pH:7.2. Redocking the cocrystal ligands of both enzymes with acarbose Glide SP served to confirm the docking studies.[60] The molecules Glide SP were docked with the target -glucosidase and -amylase.

4.4 | Molecular Dynamics Simulations

Gromacs 2021.2 version was used for the MD simulation, much like in our earlier published work.[61–63] Using the CHARMM-GUI service (https://charmm-gui.org/), the relevant input files for MD of protein-ligand complexes obtained from the glide ligand docking investigation were produced.[64,65] The protein-ligand combination was used to generate a triclinic water box using the TIP water model at 10, which was then neutralized by adding 0.15 M KCl. NVT/NPT ensemble equilibration stages with a 0.3 ns duration were carried out after 5000 steps of minimization. Two thousand frames were captured while 200 ns of MD was simulated to 2 fs. CHARMM36m force fields were used to produce topology files.[66] Trajectory analyzes were performed with gmx rms and rmsf scripts. MD animation videos were created with PyMOL Molecular Graphics System v2.5.2.

ACKNOWLEDGMENTS

The authors thank Ankara University-Scientific Research Unity for supplying the Schrödinger software purchased under grant project number BAP-21B0237004. The molecular dynamics numerical calculations reported in this paper were partially performed at TUBITAK ULAKBIM in TURKEY, High Performance and Grid Computing Center (TRUBA resources).

CONFLICTS OF INTEREST STATEMENT

The authors declare no conflicts of interest.

ORCID

Ulviye Acar Çevik http://orcid.org/0000-0003-1879-1034
Yusuf Özkay http://orcid.org/0000-0001-8815-153X
Zafer A. Kaplancıklı http://orcid.org/0000-0003-2252-0923

REFERENCES

[1] World Health Organization. *Diabetes fact sheet*. **2021**. https://www.who.int/news-room/fact-sheets/detail/diabetes
[2] M. F. Carroll, A. Gutierrez, M. Castro, D. Tsewang, D. S. Schade, *J. Clinical Endocrinol. Metab*. **2003**, *88*, 5248. https://doi.org/10.1210/jc.2003-030649
[3] E. Giovannucci, D. M. Harlan, M. C. Archer, R. M. Bergenstal, S. M. Gapstur, L. A. Habel, M. Pollak, J. G. Regensteiner, D. Yee, *Diabetes Care* **2010**, *33*, 1674. https://doi.org/10.2337/dc10-0666
[4] S. Suh, K. W. Kim, *Diabetes Metab. J*. **2011**, *35*, 193. https://doi.org/10.4093/dmj.2011.35.3.193
[5] S. K. Garg, H. Maurer, K. Reed, R. Selagamsetty, *Diabetes Obes. Metab*. **2014**, *16*, 97. https://doi.org/10.1111/dom.12124
[6] L. M. A. J. Muller, K. J. Gorter, E. Hak, W. L. Goudzwaard, F. G. Schellevis, A. I. M. Hoepelman, G. E. H. M. Rutten, *Clin. Infect. Dis*. **2005**, *41*, 281. https://doi.org/10.1086/431587
[7] S. M. Samuel, E. Varghese, S. Varghese, D. Büsselberg, *Cancer Treat. Rev*. **2018**, *70*, 98. https://doi.org/10.1016/j.ctrv.2018.08.004
[8] A. V. Aryangat, J. E. Gerich, *Vasc. Health Risk. Manag*. **2010**, *6*, 145. https://doi.org/10.2147/vhrm.s8216
[9] L. S. S., C. Raghu, A. H. A., A. P., *Carbohydr. Polym*. **2019**, *209*, 350. https://doi.org/10.1016/j.carbpol.2019.01.039
[10] B. R. Miller, H. Nguyen, C. J. Hu, C. Lin, Q. T. Nguyen, *Am. Health Drug Benefits* **2014**, *7*, 452.
[11] C. Rosak, G. Mertes, *Diabetes Metab. Syndr. Obes*. **2012**, *5*, 357. https://doi.org/10.2147/DMSO.S28340
[12] L. Zeng, G. Zhang, Y. Liao, D. Gong, *Food Funct*. **2016**, *7*, 3953. https://doi.org/10.1039/c6fo00680a
[13] S. R. Joshi, E. Standl, N. Tong, P. Shah, S. Kalra, R. Rathod, *Expert Opin. Pharmacother*. **2015**, *16*, 1959. https://doi.org/10.1517/14656566.2015.1070827
[14] V. Rani, G. Deep, R. K. Singh, K. Palle, U. C. S. Yadav, *Life Sci*. **2016**, *148*, 183. https://doi.org/10.1016/j.lfs.2016.02.002
[15] R. Pili, J. Chang, R. A. Partis, R. A. Mueller, F. J. Chrest, A. Passaniti, *Cancer Res*. **1995**, *55*, 2920.
[16] M. Saeedi, A. Hadjiakhondi, S. Nabavi, A. Manayi, *Curr. Top. Med. Chem*. **2016**, *17*, 428. https://doi.org/10.2174/1568026616666160824104655
[17] H. Y. Aboul-Enein, *Med. Chem*. **2015**, *5*, 318. https://doi.org/10.4172/2161-0444.1000280
[18] N. Kerru, L. Gummidi, S. Maddila, K. K. Gangu, S. B. Jonnalagadda, *Molecules* **2020**, *25*, 1909.
[19] M. Taha, N. H. Ismail, S. Lalani, M. Q. Fatmi, S. Atia-Tul-Wahab, S. Siddiqui, K. M. Khan, S. Imran, M. I. Choudhary, *Eur. J. Med. Chem*. **2015**, *92*, 387. https://doi.org/10.1016/j.ejmech.2015.01.009
[20] M. Özil, M. Emirik, A. Beldüz, S. Ülker, *Bioorg. Med. Chem*. **2016**, *24*, 5103. https://doi.org/10.1016/j.bmc.2016.08.024
[21] M. Özil, M. Emirik, S. Y. Etlik, S. Ülker, B. Kahveci, *Bioorg. Chem*. **2016**, *68*, 226. https://doi.org/10.1016/j.bioorg.2016.08.011
[22] T. Arshad, K. M. Khan, N. Rasool, U. Salar, S. Hussain, T. Tahir, M. Ashraf, A. Wadood, M. Riaz, S. Perveen, M. Taha, N. H. Ismail, *Med. Chem. Res*. **2016**, *25*, 2058. https://doi.org/10.1007/s00044-016-1614-y
[23] L. Dinparast, H. Valizadeh, M. B. Bahadori, S. Soltani, B. Asghari, M. R. Rashidi, *J. Mol. Struct*. **2016**, *1114*, 84. https://doi.org/10.1016/j.molstruc.2016.02.005
[24] M. Taha, N. H. Ismail, S. Imran, M. H. Mohamad, A. Wadood, F. Rahim, S. M. Saad, A. Rehman, K. M. Khan, *Bioorg. Chem*. **2016**, *65*, 100. https://doi.org/10.1016/j.bioorg.2016.02.004
[25] N. K. N. A. Zawawi, M. Taha, N. Ahmat, N. H. Ismail, A. Wadood, F. Rahim, *Bioorg. Chem*. **2017**, *70*, 184. https://doi.org/10.1016/j.bioorg.2016.12.009

[26] S. S. Bharadwaj, B. Poojary, S. K. M. Nandish, J. Kengaiah, M. P. Kirana, M. K. Shankar, A. J. Das, A. Kulal, D. Sannaningaiah, *ACS Omega* **2018**, *3*, 12562. https://doi.org/10.1021/acsomega.8b01476

[27] G. Singh, A. Singh, V. Singh, R. K. Verma, J. Tomar, R. Mall, *Med. Chem. Res*. **2020**, *29*, 1846. https://doi.org/10.1007/s00044-020-02605-5

[28] F. Peytam, G. Takalloobanafshi, T. Saadattalab, M. Norouzbahari, Z. Emamgholipour, S. Moghimi, L. Firoozpour, H. R. Bijanzadeh, M. A. Faramarzi, S. Mojtabavi, P. Rashidi-Ranjbar, S. Karima, R. Pakraad, A. Foroumadi, *Sci. Rep*. **2021**, *11*, 11911. https://doi.org/10.1038/s41598-021-91473-z

[29] S. R. Brishty, M. J. Hossain, M. U. Khandaker, M. R. I. Faruque, H. Osman, S. M. A. Rahman, *Front. Pharmacol*. **2021**, *12*, 762807. https://doi.org/10.3389/fphar.2021.762807

[30] L. M. Aroua, H. R. Almuhaylan, F. M. Alminderej, S. Messaoudi, S. Chigurupati, S. Al-mahmoud, H. A. Mohammed, *Bioorg. Chem*. **2021**, *114*, 105073. https://doi.org/10.1016/j.bioorg.2021.105073

[31] A. A. Adegboye, K. M. Khan, U. Salar, S. A. Aboaba, S. Kanwal, S. Chigurupati, I. Fatima, M. Taha, A. Wadood, J. I. Mohammad, H. Khan, S. Perveen, *Eur. J. Med. Chem*. **2018**, *150*, 248. https://doi.org/10.1016/j.ejmech.2018.03.011

[32] A. A. Akande, U. Salar, K. M. Khan, S. Syed, S. A. Aboaba, S. Chigurupati, A. Wadood, M. Riaz, M. Taha, S. Bhatia, P. Kanwal, S. Shamim, S. Perveen, *ACS Omega* **2021**, *6*, 22726. https://doi.org/10.1021/acsomega.1c03056

[33] S. Hussain, M. Taha, F. Rahim, S. Hayat, K. Zaman, N. Iqbal, M. Selvaraj, M. Sajid, M. A. Bangesh, F. Khan, K. M. Khan, N. Uddin, S. A. A. Shah, M. Ali, *J. Mol. Struct*. **2021**, *1232*, 130029. https://doi.org/10.1016/j.molstruc.2021.130029

[34] H. Kashtoh, S. Hussain, A. Khan, S. M. Saad, J. A. J. Khan, K. M. Khan, S. Perveen, M. I. Choudhary, *Bioorg. Med. Chem*. **2014**, *22*, 5454. https://doi.org/10.1016/j.bmc.2014.07.032

[35] M. Taha, N. H. Ismail, S. Imran, M. Q. B. Rokei, S. M. Saad, K. M. Khan, *Bioorg. Med. Chem*. **2015**, *23*, 4155. https://doi.org/10.1016/j.bmc.2015.06.060

[36] M. Taha, N. H. Ismail, S. Imran, A. Wadood, M. Ali, F. Rahim, A. A. Khan, M. Riaz, *RSC Adv*. **2016**, *6*, 33733. https://doi.org/10.1039/C5RA28012E

[37] M. Taha, N. H. Ismail, S. Imran, A. Wadood, F. Rahim, S. M. Saad, K. M. Khan, A. Nasir, *Bioorg. Chem*. **2016**, *66*, 117. https://doi.org/10.1016/j.bioorg.2016.04.006

[38] M. Taha, S. Imran, F. Rahim, A. Wadood, K. M. Khan, *Bioorg. Chem*. **2018**, *76*, 273. https://doi.org/10.1016/j.bioorg.2017.12.001

[39] M. Taha, F. Rahim, S. Imran, N. H. Ismail, H. Ullah, M. Selvaraj, M. T. Javid, U. Salar, M. Ali, K. M. Khan, *Bioorg. Chem*. **2017**, *74*, 30. https://doi.org/10.1016/j.bioorg.2017.07.009

[40] M. Kazmi, S. Zaib, A. Ibrar, S. T. Amjad, Z. Shafique, S. Mehsud, A. Saeed, J. Iqbal, I. Khan, *Bioorg. Chem*. **2018**, *77*, 190. https://doi.org/10.1016/j.bioorg.2017.12.022

[41] R. S. Gani, A. K. Kudva, K. Timanagouda, S. B. H. Raghuveer, S. B. H. Mujawar, S. D. Joshi, S. V. Raghu, *Bioorg. Chem*. **2021**, *114*, 105046. https://doi.org/10.1016/j.bioorg.2021.105046

[42] S. S. Hamdani, B. A. Khan, M. N. Ahmed, S. Hameed, K. Akhter, K. Ayub, T. Mahmood, *J. Mol. Struct*. **2020**, *1200*, 127085. https://doi.org/10.1016/j.molstruc.2019.127085.

[43] N. Shehzadi, K. Hussain, N. I. Bukhari, M. Islam, M. T. Khan, M. Salman, S. Z. Siddiqui, A. U. Rehman, M. A. Abbasi, *Bangl. J. Pharmacol*. **2018**, *13*, 149. http://orcid.org/0000-0001-6688-3289

[44] A. C. Maritim, R. A. Sanders, J. B. Watkins, *J. Biochem. Mol. Toxicol*. **2003**, *17*, 24. https://doi.org/10.1002/jbt.10058

[45] L. M. Aroua, H. R. Almuhaylan, F. M. Alminderej, S. Messaoudi, S. Chigurupati, S. Al-Mahmoud, H. A. Mohammed, *Bioorg. Chem*. **2021**, *114*, 105073. https://doi.org/10.1016/j.bioorg.2021.105073

[46] G. Singh, A. Singh, V. Singh, R. K. Verma, J. Tomar, R. Mall, *Med. Chem. Res*. **2020**, *29*, 1846. https://doi.org/10.1007/s00044-020-02605-5

[47] V. Claudio viegas-Junior, B. Eliezer J. Barreiro, B. Carlos Alberto Manssour Fraga, *Curr. Med. Chem*. **2007**, *14*, 1829. https://doi.org/10.2174/092986707781058805

[48] L. M. Aroua, H. R. Almuhaylan, F. M. Alminderej, S. Messaoudi, S. Chigurupati, S. Al-Mahmoud, H. A. Mohammed, *Bioorg. Chem*. **2021**, *114*, 105073. https://doi.org/10.1016/j.bioorg.2021.105073

[49] J. A. Junejo, K. Zaman, M. Rudrapal, I. Celik, E. I. Attah, *S. Afr. J. Bot*. **2021**, *143*, 164. https://doi.org/10.1016/j.sajb.2021.07.023

[50] K. Karrouchi, I. Celik, S. Fettach, T. Karthick, K. Bougrin, S. Radi, M. E. A. Faouzi, M. Ansar, R. Renjith, *J. Mol. Struct*. **2022**, *1265*, 133363. https://doi.org/10.1016/j.molstruc.2022.133363

[51] E. Yeşilçayır, İ. Çelik, H. T. Şen, S. S. Gürpınar, M. Eryılmaz, G. Ayhan -Kılcıgil, *Acta Chim. Slov*. **2022**, *69*, 419. https://doi.org/10.17344/acsi.2021.7314

[52] F. Doganc, I. Celik, G. Eren, M. Kaiser, R. Brun, H. Goker, *Eur. J. Med. Chem*. **2021**, *221*, 113545. https://doi.org/10.1016/j.ejmech.2021.113545

[53] L. Paşayeva, B. Özalp, H. Fatullayev, *J. Food Measure. Char*. **2020**, *14*, 2819. https://doi.org/10.1007/s11694-020-00527-9

[54] O. Erel, *Clin. Biochem*. **2005**, *38*, 1103. https://doi.org/10.1016/j.clinbiochem.2005.08.008

[55] G. Çetiner, U. Acar Çevik, I. Celik, H. E. Bostancı, Y. Özkay, Z. A. Kaplancıklı, *J. Mol. Struct*. **2023**, *1278*, 134920. https://doi.org/10.1016/j.molstruc.2023.134920

[56] V. Roig-Zamboni, B. Cobucci-Ponzano, R. Iacono, M. C. Ferrara, S. Germany, Y. Bourne, G. Parenti, M. Moracci, G. Sulzenbacher, *Nat. Commun*. **2017**, *8*, 1111. https://doi.org/10.1038/s41467-017-01263-3

[57] C. Gilles, J. P. Astier, G. Marchis-Mouren, C. Cambillau, F. Payan, *Eur. J. Biochem*. **1996**, *238*, 561. https://doi.org/10.1111/j.1432-1033.1996.0561z.x

[58] M. Varadi, S. Anyango, M. Deshpande, S. Nair, C. Natassia, G. Yordanova, D. Yuan, O. Stroe, G. Wood, A. Laydon, A. Žídek, T. Green, K. Tunyasuvunakool, S. Petersen, J. Jumper, E. Clancy, R. Green, A. Vora, M. Lutfi, M. Figurnov, A. Cowie, N. Hobbs, P. Kohli, G. Kleywegt, E. Birney, D. Hassabis, S. Velankar, *Nucleic Acids Res*. **2022**, *50*, D439. https://doi.org/10.1093/nar/gkab1061

[59] C. Lu, C. Wu, D. Ghoreishi, W. Chen, L. Wang, W. Damm, G. A. Ross, M. K. Dahlgren, E. Russell, C. D. Von Bargen, R. Abel, R. A. Friesner, E. D. Harder, *J. Chem. Theory Comput*. **2021**, *17*, 4291. https://doi.org/10.1021/acs.jctc.1c00302

[60] R. A. Friesner, J. L. Banks, R. B. Murphy, T. A. Halgren, J. J. Klicic, D. T. Mainz, M. P. Repasky, E. H. Knoll, M. Shelley, J. K. Perry, D. E. Shaw, P. Francis, P. S. Shenkin, *J. Med. Chem*. **2004**, *47*, 1739. https://doi.org/10.1021/jm0306430

[61] I. Celik, S. Y. Sarıaltın, T. Çoban, G. Kılcıgil, *Chem. Select* **2022**, *7*, e202201548. https://doi.org/10.1002/slct.202201548

[62] A. Işık, U. Acar Çevik, A. Karayel, I. Celik, T. Erçetin, A. Koçak, Y. Özkay, Z. A. Kaplancıklı, *SAR QSAR Environ. Res*. **2022**, *33*, 193. https://doi.org/10.1080/1062936X.2022.2041723

[63] M. J. Abraham, T. Murtola, R. Schulz, S. Páll, J. C. Smith, B. Hess, E. Lindahl, *SoftwareX*. **2015**, *1-2*, 19. https://doi.org/10.1016/j.softx.2015.06.001

[64] S. Jo, T. Kim, V. G. Iyer, W. Im, *J. Comput. Chem*. **2008**, *29*, 1859. https://doi.org/10.1002/jcc.20945

[65] B. R. Brooks, C. L. Brooks III, A. D. Mackerell Jr., L. Nilsson, R. J. Petrella, B. Roux, Y. Won, G. Archontis, C. Bartels, S. Boresch, A. Caflisch, L. Caves, Q. Cui, A. R. Dinner, M. Feig, S. Fischer, J. Gao, M. Hodoscek, W. Im, K. Kuczera, T. Lazaridis, J. Ma, V. Ovchinnikov, E. Paci, R. W. Pastor, C. B. Post, J. Z. Pu, M. Schaefer, B. Tidor, R. M. Venable, H. L. Woodcock, X. Wu, W. Yang, D. M. York, M. Karplus, *J. Comput. Chem.* **2009**, 30, 1545. https://doi.org/10.1002/jcc.21287

[66] J. Huang, S. Rauscher, G. Nawrocki, T. Ran, M. Feig, B. L. De Groot, H. Grubmüller, A. D. MacKerell, *Nature Methods* **2017**, *14*, 71. https://doi.org/10.1038/NMETH.4067

SUPPORTING INFORMATION

Additional supporting information can be found online in the Supporting Information section at the end of this article.

How to cite this article: U. Acar Çevik, I. Celik, L. Paşayeva, H. Fatullayev, H. E. Bostancı, Y. Özkay, Z. A. Kaplancıklı, *Arch. Pharm.* **2023**, e2200663. https://doi.org/10.1002/ardp.202200663